

A CRISPR-Cas system enhances envelope integrity mediating antibiotic resistance and inflammasome evasion

Timothy R. Sampson^{a,b,c}, Brooke A. Napier^{a,b,c,1,2}, Max R. Schroeder^{a,1}, Rogier Louwen^d, Jinshi Zhao^e, Chui-Yoke Chin^{b,c}, Hannah K. Ratner^{a,b,c}, Anna C. Llewellyn^{a,b,c,3}, Crystal L. Jones^{a,b,c,4}, Hamed Laroufi^f, Didier Merlin^f, Pei Zhou^e, Hubert P. Endtz^d, and David S. Weiss^{b,c,g,5}

^aDepartment of Microbiology and Immunology, Microbiology and Molecular Genetics Program, ^bEmory Vaccine Center, and ^cYerkes National Primate Research Center, Emory University, Atlanta, GA 30329; ^dDepartment of Medical Microbiology and Infectious Diseases, Erasmus Medical Center, University Medical Centre Rotterdam, Rotterdam, The Netherlands; ^eDepartment of Biochemistry, Duke University Medical Center, Durham, NC 27710; ^fDepartment of Biology, Center for Diagnostics and Therapeutics, Georgia State University, Atlanta, GA 30302; and ^gDivision of Infectious Diseases, Department of Medicine, Emory University School of Medicine, Atlanta, GA 30322

Edited by Ralph R. Isberg, Howard Hughes Medical Institute/Tufts University School of Medicine, Boston, MA, and approved June 13, 2014 (received for review December 12, 2013)

Clustered, regularly interspaced, short palindromic repeats–CRISPR associated (CRISPR-Cas) systems defend bacteria against foreign nucleic acids, such as during bacteriophage infection and transformation, processes which cause envelope stress. It is unclear if these machineries enhance membrane integrity to combat this stress. Here, we show that the Cas9-dependent CRISPR-Cas system of the intracellular bacterial pathogen *Francisella novicida* is involved in enhancing envelope integrity through the regulation of a bacterial lipoprotein. This action ultimately provides increased resistance to numerous membrane stressors, including antibiotics. We further find that this previously unappreciated function of Cas9 is critical during infection, as it promotes evasion of the host innate immune absent in melanoma 2/apoptosis associated speck-like protein containing a CARD (AIM2/ASC) inflammasome. Interestingly, the attenuation of the *cas9* mutant is complemented only in mice lacking both the AIM2/ASC inflammasome and the bacterial lipoprotein sensor Toll-like receptor 2, but not in single knockout mice, demonstrating that Cas9 is essential for evasion of both pathways. These data represent a paradigm shift in our understanding of the function of CRISPR-Cas systems as regulators of bacterial physiology and provide a framework with which to investigate the roles of these systems in myriad bacteria, including pathogens and commensals.

gene regulation | innate immune evasion

Clustered, regularly interspaced, short palindromic repeats–CRISPR associated (CRISPR-Cas) systems are adaptive bacterial defenses against foreign nucleic acids derived from bacteriophages, plasmids, and other sources (1–4). Foreign nucleic acids are targeted by direct hybridization of small CRISPR RNAs (crRNAs), which act in conjunction with conserved Cas proteins to mediate cleavage of the target. Interestingly, there is evidence that CRISPR-Cas components are up-regulated in the presence of bacteriophages or due to perturbations in the cell envelope (5–7), suggesting that CRISPR-Cas systems are induced in response to envelope stresses. Despite this up-regulation, it is unknown whether CRISPR-Cas systems function to counteract the stresses occurring at the envelope.

We demonstrated a role for components of a type II-B CRISPR-Cas system, which are encoded predominantly in pathogens and commensals (8–10), in the regulation of a membrane lipoprotein produced by the intracellular pathogen *Francisella novicida* (11). Through the action of the RNA-directed endonuclease Cas9 and two small RNAs, tracrRNA and scaRNA, the transcript for a bacterial lipoprotein (BLP; *FTN_1103*) is targeted and its stability altered, resulting in a decrease in protein production (*SI Appendix*, Fig. S1) (11). As this is the only known

direct and natural example of CRISPR-Cas-mediated endogenous gene regulation, the *F. novicida* type II-B CRISPR-Cas system represents an important model to understand how these common prokaryotic genetic elements can act as regulators to control microbial physiology.

F. novicida is capable of causing disease in a number of mammalian species, including humans (12–14). During infection, *F. novicida* must resist the action of numerous antimicrobials that are present on mucosal surfaces and within phagosomes of innate immune cells such as macrophages (15). Compared with

Significance

Increasing the integrity of the bacterial envelope is necessary to allow the successful survival of bacterial pathogens within the host and allow them to counteract damage caused by membrane-targeting antibiotics. We demonstrate that components of a clustered, regularly interspaced, short palindromic repeats–CRISPR associated (CRISPR-Cas) system, a prokaryotic defense against viruses and foreign nucleic acid, act to regulate the permeability of the bacterial envelope, ultimately providing these cells with the capability to resist membrane damage caused by antibiotics. This regulation further allows bacteria to resist detection by multiple host receptors to promote virulence. Overall, this study demonstrates the breadth of function of CRISPR-Cas systems in regulation, antibiotic resistance, innate immune evasion, and virulence.

Author contributions: T.R.S. and D.S.W. designed research; T.R.S., B.A.N., M.R.S., R.L., J.Z., C.-Y.C., H.K.R., A.C.L., C.L.J., P.Z., and H.P.E. performed research; H.L. and D.M. contributed new reagents/analytic tools; T.R.S., B.A.N., M.R.S., R.L., J.Z., C.-Y.C., H.K.R., C.L.J., P.Z., H.P.E., and D.S.W. analyzed data; B.A.N. performed the immunofluorescence staining and imaging; M.R.S. developed and executed the polymyxin B screen; R.L. and H.P.E. performed experiments with *C. jejuni*; J.Z. and P.Z. isolated and analyzed the lipid A; C.-Y.C. performed surface charge analysis; H.K.R. performed susceptibility assays; A.C.L. generated the *FTN_1254* and *FTN_0109* mutants; C.L.J. made fundamental contributions to experimental direction; T.R.S. performed all other experiments; and T.R.S. and D.S.W. wrote the paper.

The authors declare no conflict of interest.

This article is a PNAS Direct Submission.

¹B.A.N. and M.R.S. contributed equally to this work.

²Present address: Department of Microbiology and Immunology, Stanford University, Stanford, CA 94305.

³Present address: Coxiella Pathogenesis Section, Laboratory of Intracellular Parasites, Rocky Mountain Laboratories, National Institute of Allergy and Infectious Diseases, National Institutes of Health, Hamilton, MT 59840.

⁴Present address: Department of Wound Infections, Walter Reed Army Institute of Research, Silver Spring, MD 20910.

⁵To whom correspondence should be addressed. Email: david.weiss@emory.edu.

This article contains supporting information online at www.pnas.org/lookup/suppl/doi:10.1073/pnas.1323025111/-DCSupplemental.

other Gram-negative species, *F. novicida* is highly resistant to the effects of several antimicrobials, including cationic antimicrobial peptides that disrupt bacterial membranes causing lysis and death (16–18). These cationic antimicrobial peptides act similarly to polymyxin antibiotics which are often used as surrogates for their study, and *F. novicida* is also extremely resistant to polymyxins. Following phagocytosis by macrophages, *F. novicida* escapes the phagosome and replicates to high titers in the cytosol (19). Throughout this cycle, the macrophage employs numerous pattern recognition receptors to respond to *F. novicida* infection. This includes the BLP receptor Toll-like receptor 2 (TLR2), present at both the plasma membrane and in the phagosome, which initiates a proinflammatory response (20). Additionally, *F. novicida* can be recognized in the host cytosol by the absent in melanoma 2/apoptosis associated speck-like protein containing a CARD (AIM2/ASC) inflammasome (21–23). This protein complex triggers activation of the cysteine protease caspase-1, which mediates an inflammatory host cell death. Cell death results in the loss of the intracellular replicative niche for *F. novicida*, and as such, plays an important role in controlling infection. Because both TLR2 and the AIM2/ASC inflammasome are important for host defense against *F. novicida* infection, dampening the activation of these innate signaling pathways is critical for *F. novicida* pathogenesis (24–26).

We initially sought to identify genes that allow *F. novicida* to resist antimicrobials, using polymyxin for these studies. Surprisingly, we identified the CRISPR-Cas gene *cas9* as being required for *F. novicida* resistance to this membrane-targeting antibiotic. We subsequently found that *tracrRNA* and *scaRNA*, two small RNAs that function with Cas9, were also necessary for polymyxin resistance, and that this process was dependent on their ability to repress production of the FTN_1103 BLP. We further observed that this regulation was critical for the enhancement of envelope integrity, which facilitated resistance to other antimicrobials as well. This process also occurred during infection of host cells and subsequently dampened AIM2/ASC inflammasome activation. The importance of Cas9-mediated evasion of the inflammasome, as well as evasion of TLR2, in *F. novicida* pathogenesis was highlighted by the demonstration that the *cas9* deletion mutant was rescued for virulence in mice lacking both ASC and TLR2, but not either component alone. Thus, the work presented here demonstrates that CRISPR-Cas systems are capable of enhancing the integrity of the bacterial envelope, a previously unappreciated role in bacterial physiology. This promotes resistance to antimicrobials and, during infection, facilitates the evasion of multiple innate defense pathways. This represents a previously unappreciated CRISPR-Cas function that is likely relevant to numerous bacteria, including pathogenic and commensal species.

Results

Cas9 Regulatory Axis Promotes Enhancement of Envelope Integrity.

We sought to determine if CRISPR-Cas systems could enhance bacterial membrane integrity, because they are known to be up-regulated in response to nucleic acid transfer events associated with envelope stress. A genetic screen for determinants of *F. novicida* resistance to the membrane targeting antibiotic polymyxin B (details of which can be found in the *SI Appendix*, Figs. S2 and S3 and Tables S1–S3) identified the gene encoding the CRISPR-Cas endonuclease Cas9 (*FTN_0757*). The *cas9* mutant was significantly hindered in its ability to grow in the presence of polymyxin, even at doses that had little effect on the growth of WT bacteria (Fig. 1A and *SI Appendix*, Fig. S4), and was also unable to resist a lethal dose of this antimicrobial (Fig. 1B). This defect could be successfully complemented by restoration of the *cas9* gene to the deletion mutant (*SI Appendix*, Fig. S5). In contrast, mutants lacking *cas1*, *cas2*, *cas4*, or the CRISPR locus were not defective in their ability to survive in the presence of polymyxin B (*SI Appendix*, Fig. S6). Resistance to polymyxin is often mediated by alterations to the structure of lipid A in the

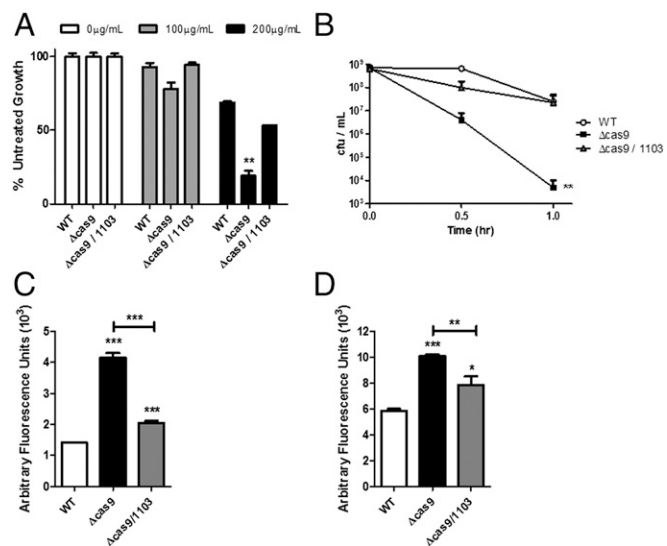


Fig. 1. The Cas9 regulatory axis is necessary for polymyxin resistance. (A) WT, *cas9*, or *cas9/1103* deletion mutants were grown overnight in both culture containing the indicated concentration of polymyxin B. Percent growth compared with untreated cultures is plotted ($n = 3$). (B) 10^9 cfu of WT, *cas9*, or *cas9/1103* deletion mutants were treated with 800 $\mu\text{g}/\text{mL}$ of polymyxin B, and cfu were enumerated at the indicated times to quantify antimicrobial killing. (C and D) WT, *cas9*, or *cas9/1103* deletion mutants were grown to midlog phase, washed, and stained with (C) propidium iodide or (D) ethidium bromide, and fluorescence was measured ($n = 3$). * $P \leq 0.05$; ** $P \leq 0.005$; *** $P \leq 0.001$.

outer membrane and an increase in surface charge. However, the *cas9* deletion mutant produced a lipid A identical to WT cells (*SI Appendix*, Fig. S7) and had similar total surface charge (*SI Appendix*, Fig. S8). Together, these data clearly demonstrate the importance of Cas9 in the enhancement of resistance against a membrane-damaging antibiotic through a mechanism independent of lipid A modifications.

Because *F. novicida* Cas9 functions with two small RNAs (*tracrRNA* and *scaRNA*; the three components are together referred to as the Cas9 regulatory system) to regulate an endogenous transcript encoding a membrane-localized BLP (FTN_1103) (11), we tested whether mutants lacking these small RNAs had a diminished ability to grow in the presence of polymyxin. *tracrRNA* and *scaRNA* deletion mutants exhibited an increase in susceptibility, similar to the *cas9* deletion strain (*SI Appendix*, Fig. S9 A and B). Furthermore, deletion of FTN_1103 from the *cas9*, *tracrRNA*, or *scaRNA* mutants restored their resistance to polymyxin to near WT levels (Fig. 1A and *SI Appendix*, Fig. S9 A and B). In addition, we observed that the Cas9 regulatory axis mutants displayed a modest increase in susceptibility to the nonionic surfactant, Triton-X, but not hydrogen peroxide (*SI Appendix*, Figs. S10 and S11). We further found that these strains were more susceptible to streptomycin and kanamycin, first-line choices for treatment of *Francisella* infection (27) (*SI Appendix*, Figs. S12 and S13), in a manner dependent on overproduction of FTN_1103. These surprising observations suggest that the regulatory action of these CRISPR-Cas components promotes resistance to multiple antimicrobials through regulation of FTN_1103.

Because we observed a marked defect in antimicrobial resistance, we sought to address whether Cas9, *tracrRNA*, and *scaRNA* promoted resistance by enhancing the integrity of the bacterial envelope. We therefore directly analyzed the permeability of the *cas9* deletion mutant by measuring its uptake of propidium iodide (PI), which fluoresces when bound to nucleic acid. The *cas9* deletion mutant demonstrated a limited, yet significant, increase in fluorescence compared with WT bacteria,

indicating that it is more permeable to PI (Fig. 1C). Importantly, similar levels of colony-forming units were recovered from the mutant and WT bacteria during this experiment (*SI Appendix, Fig. S14*), and we observed no significant difference in the ability of the strains to grow in rich or minimal media (*SI Appendix, Fig. S15*), together indicating that although envelope permeability was altered, bacterial viability was unaffected. As a further proof of principle, we performed similar experiments with the nucleic acid-staining dye ethidium bromide (EtBr) and observed a near-identical increase in fluorescence in the *cas9* mutant (Fig. 1D). Comparable effects were observed in both the *tracrRNA* and *scaRNA* deletion mutants (*SI Appendix, Fig. S16*), which also did not display an observable defect during growth in broth (*SI Appendix, Fig. S15*). Furthermore, the increased permeability of all three mutant strains could be restored to near WT levels through deletion of *FTN_1103* (Fig. 1C and D and *SI Appendix, Fig. S16*), demonstrating that overproduction of this envelope lipoprotein results in decreased envelope integrity. Thus, the Cas9 regulatory axis acts to directly enhance envelope integrity in part through regulation of a BLP and thereby mediates resistance to multiple antimicrobials.

Cas9 Regulatory Axis Promotes Enhanced Bacterial Integrity During Intracellular Infection. Because these data demonstrated a role for CRISPR-Cas components in enhancing envelope integrity during growth in broth culture, we examined whether they were necessary for a similar function during infection of macrophages, an important replicative niche for *F. novicida*. Importantly, Cas9 regulatory axis mutants and double mutants lacking *FTN_1103* survived and replicated to WT levels in macrophages (Fig. 2A and *SI Appendix, Fig. S17A*). However, during intracellular

infection we observed that *cas9*, *tracrRNA*, and *scaRNA* deletion mutants displayed an almost 10-fold increase in PI staining, a measure of membrane permeability (Fig. 2B and C and *SI Appendix, Fig. S17B and C*). Additionally, intracellular permeability to PI was dependent on *FTN_1103*, further demonstrating the importance of repression of this membrane lipoprotein for the enhancement of envelope stability during infection of host cells (Fig. 2B and C and *SI Appendix, Fig. S17B and C*).

Cas9, *tracrRNA*, and *scaRNA* Are Required for Evasion of Inflammasome Activation. Because we observed an increase in the permeability of Cas9 regulatory axis mutants during intracellular infection, we sought to determine if the lack of enhanced membrane integrity might correlate with increased recognition of bacterial components by host cytosolic receptors that activate innate immune signaling pathways. *Francisella* is recognized in the cytosol by the AIM2 inflammasome, which contains the adaptor protein ASC, and is partially activated in a TLR2-dependent manner (21–23, 28). Inflammasome activation leads to an inflammatory host cell death and loss of *Francisella*'s intracellular replicative niche. To determine if the loss of envelope integrity in the Cas9 regulatory axis mutants could result in an inability to dampen inflammasome activation, we measured cell death following infection of bone marrow-derived macrophages. Mutants lacking *cas9*, *tracrRNA*, or *scaRNA* (but not other components of the CRISPR-Cas system) displayed significantly higher levels of cytotoxicity than WT bacteria (Fig. 3A and *SI Appendix, Figs. S18 and S19*), through a signaling pathway that was partially dependent on TLR2 and completely dependent on ASC (Fig. 3A). We further found that in the absence of *FTN_1103*, cytotoxicity decreased to near WT levels (Fig. 3A and *SI Appendix, Fig. S18*), demonstrating that dysregulation of the *FTN_1103* BLP is indeed the primary factor responsible for the increased activation of ASC-dependent cell death in the Cas9 regulatory axis mutants.

To directly address whether loss of envelope integrity could lead to increased inflammasome activation, we treated WT bacteria with a sublethal dose of polymyxin B. Although this dose did not result in a loss of cellular viability (*SI Appendix, Fig. S20A*), it resulted in an increase in envelope permeability as measured by EtBr staining (*SI Appendix, Fig. S20B*), similar in magnitude to that observed in the *cas9* deletion mutant (Fig. 1C). Upon infection of macrophages, WT bacteria pretreated with polymyxin B showed significantly more cytotoxicity than untreated bacteria in a manner that was partially TLR2-dependent and completely ASC-dependent (Fig. 3B), similar to the cell death elicited by the *cas9* deletion mutant (Fig. 3A). Thus, these data directly show that loss of envelope integrity can lead to increased inflammasome activation. Along with both the increased permeability and cytotoxicity of Cas9 regulatory axis mutants, these data demonstrate that Cas9-dependent enhancement of envelope integrity acts to promote evasion of the inflammasome.

The *cas9* Mutant Is Rescued for Virulence in ASC/TLR2-Deficient Mice. *cas9* deletion mutants are severely attenuated and unable to cause lethal infection in mice (11). However, the cause of this attenuation *in vivo* is not clear. Because Cas9 is important for evasion of both the inflammasome and TLR2, we tested whether the *cas9* mutant was rescued for virulence in the absence of these innate inflammatory pathways. Mice lacking ASC alone were able to control infection by the *cas9* deletion mutant, since the bacteria were undetectable in the spleen following infection (*SI Appendix, Fig. S21A*) and were unable to cause morbidity in these mice (*SI Appendix, Fig. S21B*). Similarly, mice lacking TLR2 alone were also capable of controlling infection by the *cas9* deletion mutant (*SI Appendix, Fig. S21A and C*). We therefore generated mice lacking both of these innate immune

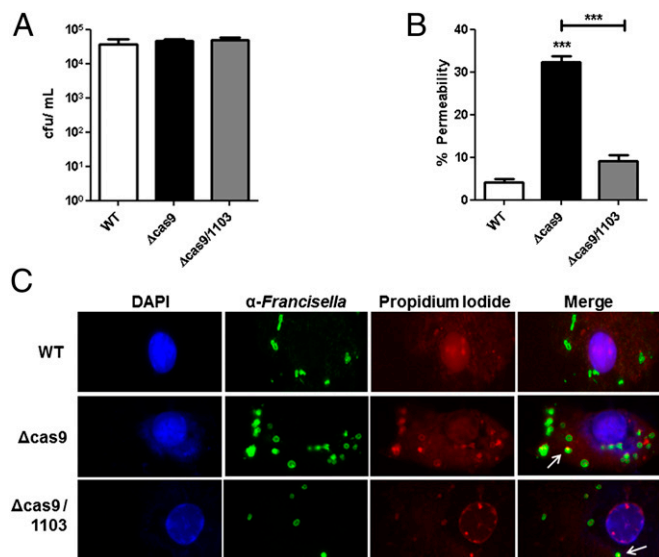


Fig. 2. Cas9 is necessary for enhanced envelope integrity during intracellular infection. (A) Bone marrow-derived macrophages were infected with WT, *cas9*, or *cas9/1103* deletion mutants at a multiplicity of infection (MOI) of 20:1 (bacteria per macrophage). At 4 h postinfection, macrophages were lysed and plated to enumerate colony-forming units. (B and C) Macrophages were infected as above, and at 4 h postinfection, were permeabilized with saponin and stained with anti-*Francisella* antibody (green), propidium iodide (nucleic acids, red), and DAPI (DNA, blue). Colocalization was determined as no less than 50% PI overlap with anti-*Francisella*. One thousand bacteria were counted per strain and quantified in B. Representative fluorescence micrographs are shown in C. Arrows indicate representative PI and anti-*Francisella* colocalization. Data are representative of at least three independent experiments in A, whereas B and C are compiled from four independent experiments. *** $P \leq 0.001$.

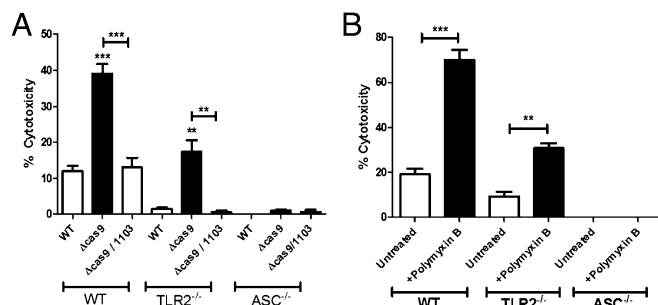


Fig. 3. Cas9 and enhanced envelope integrity promote evasion of inflammasome activation. (A) WT, TLR2^{-/-}, and ASC^{-/-} bone marrow-derived macrophages were infected with WT, *cas9*, or *cas9/1103* deletion mutants at a multiplicity of infection (MOI) of 20:1 (bacteria per macrophage). At 5.5 h postinfection, cells were assayed for cytotoxicity using the lactate dehydrogenase release assay ($n = 3$). (B) WT bacteria were untreated or pretreated for 30 min with 40 $\mu\text{g}/\text{mL}$ polymyxin B and subsequently used to infect macrophages, and cytotoxicity was measured as in A ($n = 3$). Data are representative of at least three independent experiments. ** $P \leq 0.005$; *** $P \leq 0.001$.

proteins, and infection of macrophages derived from these mice validated that the induction of both cell death and the inflammatory cytokine response by the *cas9* deletion mutant were completely abrogated (*SI Appendix, Fig. S22 A and B*). Strikingly, during infection of these mice, the *cas9* deletion mutant was significantly rescued for survival and replication (Fig. 4 *A and B* and *SI Appendix, Fig. S21A*). The level of the *cas9* mutant increased at least 3 logs in the spleen and 2–3 logs in the liver (above the limit of detection) of infected ASC/TLR2-deficient mice, reaching the levels of WT bacteria observed in WT mice (Fig. 4 *A and B*). This robust increase in bacterial burden correlated with mortality, because >90% of infected ASC/TLR2-deficient mice succumbed to infection with the *cas9* deletion

mutant (Fig. 4 *C and D*). This increase in virulence of the *cas9* mutant in ASC/TLR2-deficient mice highlights the essential role that Cas9 plays in facilitating the evasion of two distinct and critical host innate immune receptors, providing further evidence of the important roles that CRISPR-Cas systems can play in bacterial pathogenesis.

Discussion

Here, we demonstrate that the CRISPR-Cas endonuclease Cas9, working in conjunction with tracrRNA and scaRNA, is critical for enhancing the stability of the bacterial envelope and promoting resistance to polymyxin B, as well as other antibiotics. Expression of CRISPR-Cas components can be induced by bacterial envelope stress, disruptions in envelope protein localization (5), the presence of bacteriophage (6, 7), and during infection of host cells (11, 29, 30). Taken together, this suggests that CRISPR-Cas systems are induced in response to membrane stressors, and their regulatory activity can subsequently result in the enhancement of envelope integrity to promote resistance to such stressors. It is therefore tempting to speculate that the CRISPR-Cas response to envelope stress serves two distinct purposes: (i) the activation of its canonical function as the adaptive, foreign nucleic acid restriction system and (ii) the regulation of envelope structure and content to enhance the integrity of the bacterial envelope and combat membrane stress, which represents a previously unappreciated role in bacterial physiology and a shift in the understanding of these systems.

Our data demonstrate a role for CRISPR-Cas systems in promoting antibiotic resistance, whereas previous studies have focused instead on their ability to limit this process by restricting the acquisition of mobile elements, including those which carry resistance cassettes. Studies in several bacterial species revealed a correlation between increased antibiotic resistance and non-functional CRISPR-Cas systems (31–33). In fact, it has been demonstrated that acquisition of resistance traits can be restricted by CRISPR-Cas systems in vivo (34). In contrast, the

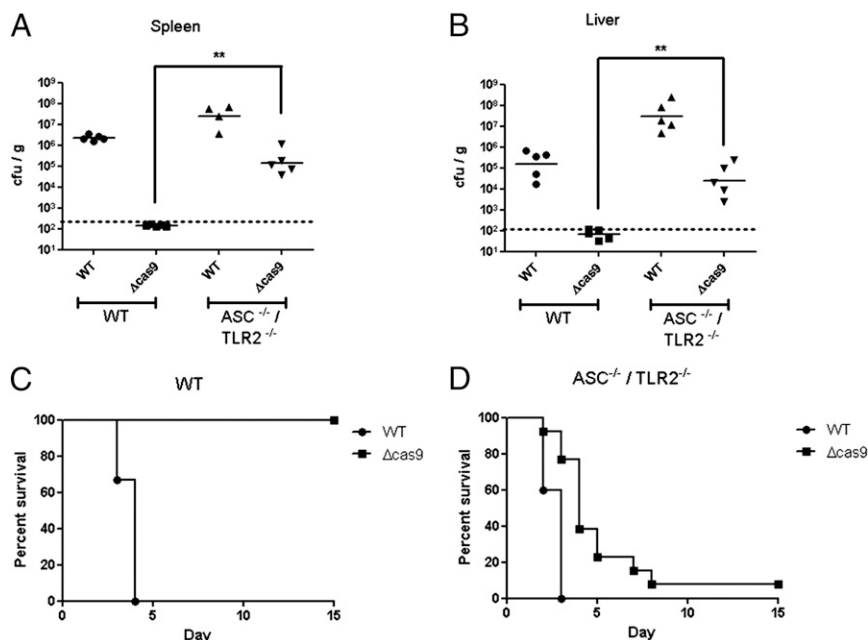


Fig. 4. A *cas9* deletion mutant is rescued for virulence in mice lacking both ASC and TLR2. (A and B) WT or ASC/TLR2-deficient mice were inoculated s.c. with 10^5 cfu of WT or the *cas9* deletion strain. Forty-eight hours postinfection, the (A) spleen and (B) liver were harvested and plated to quantify bacterial levels ($n = 5$). (C and D) Groups of 15 (C) WT or (D) ASC/TLR2-deficient mice were inoculated s.c. with 10^8 cfu of WT or *cas9* deletion strains. Mice were monitored for survival over 15 d. Data are representative of at least two independent experiments in A and B; data are compiled from three independent experiments for C and D. ** $P \leq 0.005$.

data presented here suggest that CRISPR-Cas systems with regulatory functions may provide bacteria with the capacity to resist certain antibiotics. Thus, loss of these systems in antibiotic-resistant species may have unappreciated regulatory effects leading to altered bacterial physiology (i.e., envelope structure) and enhanced susceptibility to certain antibiotics. Delineating the regulatory functions of CRISPR-Cas systems in diverse bacteria will be required to more broadly assess their potential roles as antibiotic resistance determinants.

During infection, the ability of CRISPR-Cas systems to enhance envelope integrity has important ramifications for the virulence of *F. novicida*. We demonstrate here that Cas9 regulatory axis-mediated envelope enhancement is necessary to inhibit activation of the inflammasome and host cell death. This is broadly in agreement with the idea that mutant strains with membrane defects induce increased levels of inflammasome activation (24). Furthermore, we directly demonstrate that an increase in envelope permeability induced by polymyxin B treatment leads to enhanced inflammasome activation. Because the AIM2/ASC inflammasome responds to DNA released from *Francisella*, it is likely that increased envelope stability serves to prevent the release of nucleic acid, thereby subverting inflammasome activation (21, 23, 24). It has been posited that the AIM2/ASC inflammasome has a low threshold for activation, perhaps requiring only a single bacterium to release DNA (24). Therefore, small changes in envelope integrity may have drastic effects on inflammasome activation, while not having any observable effects on a bacterial population's viability as a whole. The regulation of BLP expression by the Cas9 regulatory axis thus limits the levels of this TLR2 ligand and subsequent activation of TLR2 (11), as well as promoting enhanced envelope integrity and subversion of the inflammasome. In the absence of both ASC and TLR2, the virulence of the *cas9* mutant is significantly restored (Fig. 4 A, B, and D), demonstrating the importance of Cas9-mediated innate immune evasion in the ability of *F. novicida* to cause disease.

Although *F. novicida* is the only known bacterial species in which Cas9 plays a clearly demonstrated regulatory role, it is likely that Cas9-dependent regulation contributes to the virulence of other pathogens encoding this protein including *Streptococcus* spp., *Legionella pneumophila*, *Listeria monocytogenes*, *Staphylococcus aureus*, and *Haemophilus parainfluenzae* (8, 9, 11, 29). In fact, a role for Cas9 in controlling virulence traits has been demonstrated in *Neisseria meningitidis* and *Campylobacter jejuni*. Each has been observed to require Cas9 for both invasion and replication in eukaryotic cells (11, 35). In addition, both of these species require Cas9 to attach to host cells, further supporting the hypothesis that CRISPR-Cas systems can have effects on the bacterial envelope (11, 35). Interestingly, we have additionally observed defects in the *C. jejuni* envelope in the absence of Cas9. A *cas9* deletion mutant in *C. jejuni* displays an increase in envelope permeability, similar to that observed in *F. novicida* (SI Appendix, Fig. S23A), and is significantly more sensitive to erythromycin, a first-line treatment for invasive campylobacteriosis (SI Appendix, Fig. S23B) (36). Therefore, although it is yet unknown how Cas9 may function as a regulator in *C. jejuni*, it is clear that these findings represent a broader role for Cas9 systems in modulating this important aspect of bacterial physiology.

CRISPR-Cas systems have more broadly been linked to other processes that involve the bacterial envelope and extracellular structures. For instance, the type I CRISPR-Cas system in *Pseudomonas aeruginosa* is capable of modulating biofilm formation (37, 38), and the type I system in *Myxococcus xanthus* is an essential component in regulating the development of fruiting bodies (39–41). These examples provide further support for a broader CRISPR-Cas function in the modification and regulation of the envelope and extracellular structures, extending beyond those organisms that encode Cas9. This unappreciated

role for CRISPR-Cas systems would allow the myriad bacterial species encoding them to respond to envelope stresses that occur as a result of not only bacteriophage attack but also infection of host cells and exposure to other environmental conditions.

Experimental Procedures

Bacterial Manipulations. *F. novicida* strain U112 and all derivatives used in this study were routinely grown at 37 °C with aeration in tryptic soy broth (TSB) supplemented with 0.2% L-cysteine (BD Biosciences), or on tryptic soy agar plates supplemented with 0.1% L-cysteine. Cas9 regulatory axis deletion mutants and complementation strains were described previously (11, 42). *FTN_1254* and *FTN_0109* mutants were constructed by allelic exchange as described previously (43, 44) using primers in SI Appendix, Table S3.

Polymyxin Treatments. The indicated strains were grown overnight and subsequently diluted to an OD₆₀₀ of 0.03 in Mueller-Hinton/cation-adjusted broth with 0.2% L-cysteine containing the specified doses of polymyxin B (USB Corporation). Following overnight growth at 37 °C with aeration, OD₆₀₀ was measured and used to calculate the percent growth compared with the growth of the strain in media alone. For the killing assay, cultures were treated with 800 µg/mL of polymyxin B, incubated at 37 °C with aeration, and plated for colony-forming units at the indicated time points. For sublethal treatments with polymyxin B, bacterial cultures were washed once and resuspended in media containing 40 µg/mL polymyxin B for 30 min. Treated cells were subsequently washed twice before preparing for infections as described below.

In Vitro Permeability. The indicated strains were grown overnight and subsequently subcultured 1:50 in TSB and grown to an OD₆₀₀ of ~0.8–0.9. Cells were washed twice in 50 mM phosphate buffer and resuspended in 50 mM phosphate buffer containing 30 µg/mL EtBr (Fisher Scientific) or 200 µM PI (Life Technologies). Fluorescence was measured immediately in a Biotek Synergy Mx plate reader using an excitation of 250 nm and emission of 605 nm for EtBr or excitation of 534 nm and emission of 617 nm for PI, correcting with samples lacking bacteria.

Macrophage Culture and Infection. Murine bone marrow-derived macrophages were prepared from WT C57BL/6 mice or the indicated knockout strains and cultured as described previously (42). Macrophages were seeded overnight and infected with overnight cultures of the indicated bacterial strains at a MOI of 20:1 bacteria per macrophage. Plates were centrifuged for 15 min at 335 × g at room temperature to promote bacterial uptake. Infected macrophages were incubated for 30 min at 37 °C and washed twice before adding DMEM containing 10 µg/mL gentamicin.

Intracellular Permeability. WT murine bone marrow-derived macrophages were seeded onto glass coverslips and infected as above. At 4 h postinfection, macrophages were gently permeabilized for 15 min at room temperature with 0.1% saponin/3% (wt/vol) BSA in PBS. Cells were first stained with 2.6 µM PI and chicken-anti-*F. novicida* antibody (a kind gift from Denise Monack, Stanford University) for 12 min at 37 °C. Following washing, cells were fixed with 4% (vol/vol) paraformaldehyde and incubated with FITC-labeled anti-chicken antibody. Coverslips were mounted onto glass slides with SlowFade Gold reagent with DAPI (Life Technologies). Slides were imaged on a Zeiss AxioScope Z.1 microscope and a Zeiss Imager 2.1 camera. Images were analyzed with Velocity 5.5 software (Perkin-Elmer). Colocalization was determined by no less than 50% overlap between PI and *Francisella*-positive cells, and 1,000 cells were counted for each strain.

Cytotoxicity Assays. Murine bone marrow-derived macrophages prepared from the indicated mice were infected with bacterial strains as described above. At 5.5 h postinfection, supernatants were collected and assayed for levels of lactate dehydrogenase using the nonradioactive cytotoxicity assay kit (Promega).

Murine Infections. ASC^{-/-} and TLR2^{-/-} C57BL/6 mice were a generous gift from Bali Pulendran, Emory Vaccine Center, Atlanta (with much appreciated assistance from Paul Hakimpour) and were bred together to generate mice deficient in both ASC and TLR2. Mice were bred and kept under specific-pathogen free conditions in filter-top cages at Yerkes National Primate Center, Emory University, and provided food and water ad libitum. For bacterial burden assays, female WT or ASC/TLR2-deficient mice (of 8–10 wk of age) were infected s.c. with 2 × 10⁵ cfu of the indicated bacterial strains in sterile PBS. At 48 h postinfection, liver and spleen were harvested,

weighed, and homogenized in PBS, and serial dilutions were plated to enumerate colony-forming units. For survival experiments, mice were infected with 10^8 cfu s.c. and monitored for signs of illness. Mice were killed when they appeared moribund. All experimental procedures were approved by the Emory University Institutional Animal Care and Use Committee (Protocol #069-2008Y).

Statistics. Two-tailed, Student *t* tests were performed to analyze pairs of data as indicated, excluding the experiments in Fig. 4 A and B, which were analyzed with the Mann–Whitney test.

1. Richter C, Chang JT, Fineran PC (2012) Function and regulation of clustered regularly interspaced short palindromic repeats (CRISPR) / CRISPR associated (Cas) systems. *Virus* 4(10):2291–2311.
2. Fineran PC, Charpentier E (2012) Memory of viral infections by CRISPR-Cas adaptive immune systems: Acquisition of new information. *Virology* 434(2):202–209.
3. Sorek R, Lawrence CM, Wiedenheft B (2013) CRISPR-mediated adaptive immune systems in bacteria and archaea. *Annu Rev Biochem* 82:237–266.
4. Barrangou R, Marraffini LA (2014) CRISPR-Cas systems: Prokaryotes upgrade to adaptive immunity. *Mol Cell* 54(2):234–244.
5. Perez-Rodriguez R, et al. (2011) Envelope stress is a trigger of CRISPR RNA-mediated DNA silencing in *Escherichia coli*. *Mol Microbiol* 79(3):584–599.
6. Quax TE, et al. (2013) Massive activation of archaeal defense genes during viral infection. *J Virol* 87(15):8419–8428.
7. Young JC, et al. (2012) Phage-induced expression of CRISPR-associated proteins is revealed by shotgun proteomics in *Streptococcus thermophilus*. *PLoS ONE* 7(5): e38077.
8. Chylinski K, Le Rhun A, Charpentier E (2013) The tracrRNA and Cas9 families of type II CRISPR-Cas immunity systems. *RNA Biol* 10(5):726–737.
9. Chylinski K, Makarova KS, Charpentier E, Koonin EV (2014) Classification and evolution of type II CRISPR-Cas systems. *Nucleic Acids Res*, 10.1093/nar/gku241.
10. Schunder E, Rydzewski K, Grunow R, Heuner K (2013) First indication for a functional CRISPR/Cas system in *Francisella tularensis*. *Int J Med Microbiol* 303(2):51–60.
11. Sampson TR, Saroj SD, Llewellyn AC, Tzeng YL, Weiss DS (2013) A CRISPR/Cas system mediates bacterial innate immune evasion and virulence. *Nature* 497(7448):254–257.
12. Hand J, Scott-Waldron C, Balsamo G (2012) Outbreak of *Francisella novicida* infections among occupants at a long-term residential facility - Louisiana, April–July, 2011. *Louisiana Morbidity Rep* 23(1):1–6.
13. Birdsall DN, et al. (2009) *Francisella tularensis* subsp. *novicida* isolated from a human in Arizona. *BMC Res Notes* 2:1–6.
14. Leelaporn A, Yongyod S, Limsrivanchakorn S, Yungyuen T, Kiratisin P (2008) *Francisella novicida* Bacteremia, Thailand. *Emerg Infect Dis* 14(12):1935–1937.
15. Jones CL, et al. (2012) Subversion of host recognition and defense systems by *Francisella* spp. *Microbiol Mol Biol Rev* 76(2):383–404.
16. Han S, Bishop BM, van Hoek ML (2008) Antimicrobial activity of human beta-defensins and induction by *Francisella*. *Biochem Biophys Res Commun* 371(4):670–674.
17. Mohapatra NP, et al. (2007) Identification of an orphan response regulator required for the virulence of *Francisella* spp. and transcription of pathogenicity island genes. *Infect Immun* 75(7):3305–3314.
18. Urban C, Tiruvury H, Mariano N, Colon-Urban R, Rahal JJ (2011) Polymyxin-resistant clinical isolates of *Escherichia coli*. *Antimicrob Agents Chemother* 55(1):388–389.
19. Golovliov I, Baranov V, Krocova Z, Kovarova H, Sjöstedt A (2003) An attenuated strain of the facultative intracellular bacterium *Francisella tularensis* can escape the phagosome of monocytic cells. *Infect Immun* 71(10):5940–5950.
20. Cole LE, et al. (2010) Phagosomal retention of *Francisella tularensis* results in TIRAP/Mal-independent TLR2 signaling. *J Leukoc Biol* 87(2):275–281.
21. Fernandes-Alnemri T, et al. (2010) The AIM2 inflammasome is critical for innate immunity to *Francisella tularensis*. *Nat Immunol* 11(5):385–393.
22. Jones JW, et al. (2010) Absent in melanoma 2 is required for innate immune recognition of *Francisella tularensis*. *Proc Natl Acad Sci USA* 107(21):9771–9776.
23. Rathinam VA, et al. (2010) The AIM2 inflammasome is essential for host defense against cytosolic bacteria and DNA viruses. *Nat Immunol* 11(5):395–402.
24. Peng K, Broz P, Jones J, Joubert LM, Monack D (2011) Elevated AIM2-mediated pyroptosis triggered by hypercytotoxic *Francisella* mutant strains is attributed to increased intracellular bacteriolysis. *Cell Microbiol* 13(10):1586–1600.
25. Jones CL, Sampson TR, Nakaya HI, Pulendran B, Weiss DS (2012) Repression of bacterial lipoprotein production by *Francisella novicida* facilitates evasion of innate immune recognition. *Cell Microbiol* 14(10):1531–1543.
26. Mariathasan S, Weiss DS, Dixit VM, Monack DM (2005) Innate immunity against *Francisella tularensis* is dependent on the ASC/caspase-1 axis. *J Exp Med* 202(8): 1043–1049.
27. World Health Organization (2007) WHO Guidelines on Tularaemia. *WHO Library Cataloguing-in Publication Data* (World Health Organization, Geneva), 978 92 4 154737 6.
28. Jones CL, Weiss DS (2011) TLR2 signaling contributes to rapid inflammasome activation during *F. novicida* infection. *PLoS ONE* 6(6):e20609.
29. Louwen R, Staals RH, Endtz HP, van Baaren P, van der Oost J (2014) The role of CRISPR-Cas systems in virulence of pathogenic bacteria. *Microbiol Mol Biol Rev* 78(1): 74–88.
30. Gunderson FF, Cianciotto NP (2013) The CRISPR-associated gene cas2 of *Legionella pneumophila* is required for intracellular infection of amoebae. *MBio* 4(2): e00074–e13.
31. Palmer KL, Gilmore MS (2010) Multidrug-resistant enterococci lack CRISPR-cas. *MBio* 1(4):e00227–e10.
32. Dang TN, et al. (2013) Uropathogenic *Escherichia coli* are less likely than paired fecal *E. coli* to have CRISPR loci. *Infect Genet Evol* 19:212–218.
33. Burley KM, Sedgley CM (2012) CRISPR-Cas, a prokaryotic adaptive immune system, in endodontic, oral, and multidrug-resistant hospital-acquired *Enterococcus faecalis*. *J Endod* 38(11):1511–1515.
34. Bikard D, Hatoum-Aslan A, Mucida D, Marraffini LA (2012) CRISPR interference can prevent natural transformation and virulence acquisition during in vivo bacterial infection. *Cell Host Microbe* 12(2):177–186.
35. Louwen R, et al. (2013) A novel link between *Campylobacter jejuni* bacteriophage defence, virulence and Guillain-Barré syndrome. *Eur J Clin Microbiol Infect Dis* 32(2): 207–226.
36. Allos BM (2001) *Campylobacter jejuni* infections: Update on emerging issues and trends. *Clin Infect Dis* 32(8):1201–1206.
37. Cady KC, O’Toole GA (2011) Non-identity-mediated CRISPR-bacteriophage interaction mediated via the Csy and Cas3 proteins. *J Bacteriol* 193(14):3433–3445.
38. Zegans ME, et al. (2009) Interaction between bacteriophage DMS3 and host CRISPR region inhibits group behaviors of *Pseudomonas aeruginosa*. *J Bacteriol* 191(1): 210–219.
39. Viswanathan P, Murphy K, Julien B, Garza AG, Kroos L (2007) Regulation of dev, an operon that includes genes essential for *Myxococcus xanthus* development and CRISPR-associated genes and repeats. *J Bacteriol* 189(10):3738–3750.
40. Boysen A, Ellehaug E, Julien B, Søgaard-Andersen L (2002) The DevT protein stimulates synthesis of FruA, a signal transduction protein required for fruiting body morphogenesis in *Myxococcus xanthus*. *J Bacteriol* 184(6):1540–1546.
41. Thöny-Meyer L, Kaiser D (1993) devR5, an autoregulated and essential genetic locus for fruiting body development in *Myxococcus xanthus*. *J Bacteriol* 175(22):7450–7462.
42. Weiss DS, et al. (2007) In vivo negative selection screen identifies genes required for *Francisella* virulence. *Proc Natl Acad Sci USA* 104(14):6037–6042.
43. Brotcke A, et al. (2006) Identification of MglA-regulated genes reveals novel virulence factors in *Francisella tularensis*. *Infect Immun* 74(12):6642–6655.
44. Anthony LS, Gu MZ, Cowley SC, Leung WW, Nano FE (1991) Transformation and allelic replacement in *Francisella* spp. *J Gen Microbiol* 137(12):2697–2703.

Supplemental Results and Discussion

Francisella species are extremely resistant to polymyxin in comparison to other bacteria. We therefore set out to identify genes necessary for *F. novicida* polymyxin resistance. We initiated a screen of 470 transposon mutants from a library (1) representing 229 genes that have previously been identified as necessary for virulence *in vivo* and/or intracellular replication in mammalian cells. Each mutant was grown overnight in the presence of polymyxin B, and compared to wild-type. Mutants that failed to reach at least 75% of wild-type growth were deemed to have mutations in genes required for complete fitness in the presence of polymyxin (Supplemental Tables 1 and 2).

We identified 120 genes as playing roles in *F. novicida* resistance to polymyxin. The majority of these are categorized as having Unknown Function by COG analysis, while the remainder are primarily grouped into pathways necessary for the generation of envelope structures or within metabolic pathways that can act upstream of envelope biogenesis and modification (Supplemental Figure 2). Resistance to polymyxin is often mediated by alterations to the structure of lipid A and O-antigen, components of lipopolysaccharide (LPS) in the bacterial outer membrane. Notably, we identified *FTN_0544*, *FTN_0545*, and *lpxE* which have roles in lipid A modification and have previously been implicated in polymyxin resistance (2-4), providing validation for the results of the screen (Supplemental Table 1). Additionally, *wbtD*, *wbtF*, and *wbtH*, which are part of the O-antigen biosynthetic machinery were also identified (Supplemental Table 1)(5). To further confirm the results of the screen, we generated deletion mutants in two genes encoding proteins of unknown function, *FTN_0109* and *FTN_1254*. These deletion mutants demonstrated a significant decrease in polymyxin resistance compared to wild-type, providing additional support for screen's validity (Supplemental Figure 3).

In addition to a number of genes known to be involved in the biogenesis or modification of envelope structures, and numerous genes encoding hypothetical proteins, the screen also implicated numerous potential metabolic pathways in mediating polymyxin resistance (Supplemental Table 1 and

Supplemental Figure 2). These pathways may be involved in creating necessary precursors for envelope structures, and/or increasing metabolic output, allowing sufficient energy to resist and repair damage induced by polymyxin. In either case, the results suggest an important interplay between the metabolic status of the bacterial cell and its ability to resist the action of polymyxin. It is important to note that this screen does not differentiate between mutant strains which failed to grow in the presence of polymyxin, mutant strains which can replicate in polymyxin but subsequently are killed, and those mutant strains which are actively killed more effectively by polymyxin. However, this broad screen of 229 genes already implicated in *Francisella* virulence allows the foundation for future studies to determine their precise contribution to polymyxin resistance and virulence.

Supplemental Methods

Screen for polymyxin resistance determinants

Four hundred and seventy transposon mutants, representing 229 genes were obtained from the *Francisella* two-allele transposon mutant library (1, 6). Each transposon mutant was grown overnight in a well of a 96 well plate containing cation-adjusted Mueller Hinton broth (MH/C-A) with 0.2% L-cysteine (BD Biosciences). Subsequently, each mutant was diluted to an OD₆₀₀ of 0.03 in MH/C-A containing 100µg/mL of polymyxin B (USB Corporation, Cleveland, OH). Following overnight growth at 37°C with aeration, the OD₆₀₀ was measured and used to calculate the percent growth compared to wild-type bacteria. Strains that grew to an OD₆₀₀ of less than 75% than that of wild-type were deemed to have increased sensitivity.

Bacterial growth kinetics.

The indicated strains were grown overnight and subsequently diluted to an OD₆₀₀ of 0.03 in TSB with 0.2% L-cysteine or Chamberlain's Defined Media (CDM). Subcultures were placed at 37°C with aeration in a Biotek Synergy Mx plate reader and OD₆₀₀ was measured each hour for 15 hours.

Lipid A isolation and analysis.

Total lipid A was isolated from the indicated strains as described previously (2). Lipid A was analyzed by LC/MS as described previously (2). Briefly, LC/MS of lipids was performed using a Shimadzu LC system coupled to a QSTAR XL quadrupole time-of-flight tandem mass spectrometer.

Surface charge analysis by zeta potential

Zeta electrokinetic potentials of the indicated strains were calculated as described previously (2). Briefly, bacteria were subcultured and grown to OD₆₀₀ = 1.0, and subsequently washed and resuspended at a 5× concentration in 20 mM potassium chloride. Twenty microlitres of the concentrated bacteria were added to 3.2 ml of 20 mM potassium chloride in the zeta potential electrokinetic cuvette from Brookhaven

Instruments Corporation (BIC, Holtsville, NY). The bacterial cell sizes and zeta electrokinetic potentials were measured using the 90Plus size and zeta potential analyser (BIC). Data were analysed using BIC Zeta Potential Analyser Software Version 5.20, which corrects for bacterial cell size.

Antimicrobial resistance.

The indicated strains were grown overnight and subsequently diluted to an OD₆₀₀ of 0.03 in MH/C-A with 0.2% L-cysteine containing the specified doses of Triton X (Fisher Scientific, Pittsburgh, PA), hydrogen peroxide (Fisher Scientific, Pittsburgh, PA), kanamycin (Teknova, Hollister, CA), and streptomycin (Teknova). Following overnight growth at 37°C with aeration, OD₆₀₀ was measured and used to calculate the percent growth compared to the growth of the strain in media alone.

Intracellular survival.

Murine bone marrow-derived macrophages were infected as described in the Experimental Procedures with the indicated bacterial strains. At 4 hours post infection, macrophages were lysed with 1% saponin. Lysates were serially diluted in PBS and plated onto TSA containing 0.1% cysteine to enumerate colony forming units.

Campylobacter manipulations and experiments

The GB11 (wild-type) and its cognate $\Delta cas9$ deletion mutant have been described previously (7). Strains were routinely grown on Columbia blood agar plates containing 7% sheep blood (Becton Dickinson, Breda, The Netherlands), supplemented with vancomycin (Sigma-Aldrich, Zwijndrecht, The Netherlands) and chloramphenicol (Sigma-Aldrich) under micro-aerophilic conditions at 37°C using anaerobic jars and an Anoxomat (Mart Microbiology B.V., Drachten, The Netherlands). To measure bacterial permeability, plate-grown bacteria were recovered, washed in PBS, and diluted to a concentration of 7.5×10^7 cfu/mL in PBS containing 30 µg/mL ethidium bromide (Sigma-Aldrich). Fluorescence was measured immediately in a Fluostar Optima plate reader (BMG Labtech) using an excitation of 250nm

and an emission of 605nm. Erythromycin susceptibility was determined using an Epsilometer-test (bioMérieux, Zaltbommel, The Netherlands). Bacteria were diluted to a 1 MacFarland suspension, swabbed onto Columbia blood agar plates, and an E-test deposited. Plates were incubated overnight, as described above, and at 24 hours the MIC was determined.

Supplemental Figure Legends

Supplemental Figure 1. Model of the Cas9/dual RNA complex mediating *FTN_1103* repression.

Cas9 associates with two small RNAs, tracrRNA and scaRNA. This complex is then targeted to the *FTN_1103* transcript, encoding a bacterial lipoprotein (BLP), and ultimately mediates the repression of BLP production by altering the stability of its mRNA. Since BLP can be recognized by TLR2, leading to a proinflammatory innate immune response, the ability of Cas9 to act as a regulatory element against this transcript is critical for *Francisella* evasion of the innate immune response.

Supplemental Figure 2. COG categories of genes identified as being involved in polymyxin B

resistance. COG categories were assigned to each locus identified within the screen as defined by the *Francisella novicida* U112 genome database through NCBI (Accession #: NC_008601.1). Quantities of each COG category were plotted as percent of all categories identified within the screen.

Supplemental Figure 3. *FTN_1254* and *FTN_0109* contribute to *F. novicida* polymyxin resistance.

Wild-type (WT), *FTN_0544*, *FTN_1254*, or *FTN_0109* deletion mutants were grown overnight in TSB with or without polymyxin B (200 ug/mL). Percent growth compared to untreated cultures is plotted (n=3). **, $p \leq 0.005$, ***, $p \leq 0.001$.

Supplemental Figure 4. Growth kinetics of the *cas9* deletion mutant in the presence of polymyxin B.

Overnight cultures of wild-type (WT; circles) or the *cas9* deletion mutant (squares) were diluted to an OD₆₀₀ of ~0.03 into the media containing indicated doses of polymyxin B in a 96-well plate. Cultures were incubated at 37°C with aeration in a Biotek Synergy Mx plate reader and OD₆₀₀ was measured each hour for 18 hours (n=3).

Supplemental Figure 5. Complementation of the *cas9* deletion mutant restores polymyxin

resistance. Wild-type (WT), *cas9* deletion mutant, or a *cas9*:complement strain were grown overnight

with or without polymyxin B (200 ug/mL). Percent growth compared to untreated cultures is plotted (n=3). **: $p \leq 0.005$.

Supplemental Figure 6. Other *cas* genes are not involved in polymyxin resistance. Wild-type (WT) or deletion mutants in the indicated *cas* genes were grown overnight with or without polymyxin B (400 ug/mL). Percent growth compared to untreated cultures is plotted (n=3). **: $p \leq 0.005$

Supplemental Figure 7. Cas9 is not involved in modification of lipid A. Total lipid A was analyzed by LC/MS from wild-type (WT), the *cas9* deletion mutant, or the *cas9/1103* double deletion strain.

Supplemental Figure 8. Cas9 is not involved in alteration of cell surface charge. Cultures of wild-type (WT), the *cas9* deletion mutant, or the *cas9/1103* double deletion strain were subjected to zeta electrokinetic potential analysis. Data presented for each strain is pooled from 3 independent cultures, with multiple technical replicates.

Supplemental Figure 9. *FTN_1103* regulation by *tracrRNA* and *scaRNA* is necessary for polymyxin resistance. (A) Wild-type (WT), *tracrRNA* or *tracrRNA/1103* deletion mutants, or (B) WT, *scaRNA* or *scaRNA/1103* deletion mutants, were grown overnight in TSB containing the indicated concentrations of polymyxin B. Percent growth compared to untreated cultures is plotted (n=3). Data presented was generated during the same experiment as Figures 1a, b, utilizing the same controls, and plotted separately for clarity. **: $p \leq 0.005$.

Supplemental Figure 10. Cas9 regulatory axis provides resistance to Triton X. (A) Wild-type (WT), *cas9* and *cas9/1103* deletion mutants, (B) *tracrRNA* and *tracrRNA/1103* deletion mutants, or (C) *scaRNA* and *scaRNA/1103* deletion mutants were grown overnight in TSB, in the presence or absence of the non-ionic detergent Triton X (0.0125%). Percent growth compared to untreated cultures is plotted (n=3). Data

presented was generated during the same experiment, utilizing the same controls, and plotted separately for clarity. *; $p \leq 0.05$.

Supplemental Figure 11. Cas9 regulatory axis is not required for resistance to hydrogen peroxide.

(A) Wild-type (WT), *cas9* and *cas9/1103* deletion mutants, (B) WT, *tracrRNA* and *tracrRNA/1103* deletion mutants, or (C) WT, *scaRNA* and *scaRNA/1103* deletion mutants were grown overnight in TSB containing the indicated concentrations of hydrogen peroxide. Percent growth compared to untreated cultures is plotted (n=3). Data presented was generated during the same experiment, utilizing the same controls, and plotted separately for clarity. * $p > 0.05$.

Supplemental Figure 12. Cas9 regulatory axis is required for resistance to kanamycin. Wild-type (WT), *cas9*, *cas9/1103*, *tracrRNA*, *tracrRNA/1103*, *scaRNA*, and *scaRNA/1103* deletion mutants were grown overnight in TSB containing the indicated concentrations of kanamycin. Percent growth compared to untreated cultures is plotted (n=3). * $p > 0.05$, ***; $p \leq 0.001$.

Supplemental Figure 13. Cas9 regulatory axis is required for resistance to streptomycin. Wild-type (WT), *cas9*, *cas9/1103*, *tracrRNA*, *tracrRNA/1103*, *scaRNA*, and *scaRNA/1103* deletion mutants were grown overnight in TSB containing the indicated concentrations of streptomycin. Percent growth compared to untreated cultures is plotted (n=3). * $p > 0.05$.

Supplemental Figure 14. *cas9* mutant does not have altered viability during growth in broth. Prior to propidium iodide staining (Figure 1c), wild-type (WT), *cas9*, or *cas9/1103* deletion mutants were grown to mid-log phase in TSB, washed and plated to enumerate colony forming units (n=3).

Supplemental Figure 15. Cas9 regulatory axis mutants exhibit wild-type growth kinetics in rich or synthetic media. Wild-type (WT), *cas9*, *tracrRNA*, *scaRNA*, *cas9/1103*, *tracrRNA/1103* and

scaRNA/1103 deletion mutants were grown in (A) TSB or (B) Chamberlain's defined media (CHB) for 15 hours, and OD₆₀₀ was measured every hour (n=3).

Supplemental Figure 16. *FTN_1103* regulation by tracrRNA and scaRNA is necessary for enhanced envelope integrity. Wild-type (WT), tracrRNA, tracrRNA/1103, scaRNA, or scaRNA/1103 deletion mutants were grown to mid-log phase, washed, and stained with ethidium bromide. Fluorescence was measured at excitation 250nm and emission 605nm (n=3). **, $p \leq 0.005$, ***, $p \leq 0.001$.

Supplemental Figure 17. *FTN_1103* regulation by tracrRNA and scaRNA is necessary for enhanced envelope integrity during intracellular infection. (A) Bone marrow-derived macrophages were infected with wild-type (WT), tracrRNA, tracrRNA/1103, scaRNA, or scaRNA/1103 deletion mutants at a multiplicity of infection (MOI) of 20:1 (bacteria per macrophage). At 4 hours post infection, macrophages were permeabilized with saponin and lysates were plated to enumerate intracellular bacterial levels (n=3). (B) Macrophages were infected as above, and at 4 hours post infection, macrophages were permeabilized with saponin and stained with anti-*Francisella* antibody (green), and propidium iodide (nucleic acids; red). Co-localization was quantified as no less than 50% PI overlap with *Francisella*, and 1,000 bacteria were counted for each strain. (C) Representative fluorescence micrographs of WT, tracrRNA, tracrRNA/1103, scaRNA, or scaRNA/1103 deletion mutants. DAPI (DNA; blue), anti-*Francisella* antibody (green), and propidium iodide (nucleic acids; red). Arrows indicate representative PI and anti-*Francisella* co-localization. **, $p \leq 0.005$, ***, $p \leq 0.001$.

Supplemental Figure 18. *FTN_1103* regulation by tracrRNA and scaRNA promotes evasion of the inflammasome. Wild-type (WT), ASC^{-/-}, and TLR2^{-/-}, knockout macrophages were infected with WT, tracrRNA, tracrRNA/1103, scaRNA, or scaRNA/1103 deletion mutants at a multiplicity of infection (MOI) of 20:1. At 5.5 hours post infection, cells were assayed for cytotoxicity through LDH release (n=3). *, $p \leq 0.05$, **, $p \leq 0.005$, ***, $p \leq 0.001$.

Supplemental Figure 19. Other CRISPR/Cas components are not required for evasion of the inflammasome. Wild-type bone marrow-derived macrophages were infected with wild-type (WT), *cas9*, *cas1*, *cas2*, *cas4*, tracrRNA, crRNA, or scaRNA deletion mutants at a multiplicity of infection (MOI) of 20:1. At 5.5 hours post infection, cells were assayed for cytotoxicity through LDH release (n=3). ***, $p \leq 0.001$.

Supplemental Figure 20. Sublethal treatment with polymyxin induces increased permeability without loss of bacterial viability. Wild-type bacteria were treated with 40 μ g/mL polymyxin B for 30min, at 37°C with aeration. (A) Treated and untreated cultures were plated and colony forming units enumerated. (B) Treated and untreated cultures were grown to mid-log phase, washed, and stained with ethidium bromide and fluorescence measured (n=3). ***, $p \leq 0.001$.

Supplemental Figure 21. Virulence of the *cas9* mutant is not restored in ASC^{-/-} or TLR2^{-/-} mice. (A) Wild-type (WT), ASC^{-/-}, TLR2^{-/-}, or ASC/TLR2-deficient mice were inoculated subcutaneously with 10⁵ cfu of the *cas9* deletion strain. Forty-eight hours post infection, spleens were harvested and plated to quantify bacterial levels (n=5). (B, C) Groups of 5 (B) WT or TLR2^{-/-} and (C) WT or ASC^{-/-} mice were inoculated subcutaneously with 10⁸ cfu of WT or *cas9* deletion strains. Mice were monitored for survival over 20 days. **, $p \leq 0.005$.

Supplemental Figure 22. ASC and TLR2 control inflammasome activation and cytokine response against *cas9* deletion mutants. (A) Wild-type (WT), TLR2^{-/-}, ASC^{-/-} and ASC/TLR2-deficient bone marrow-derived macrophages were infected with wild-type (WT), *cas9*, or *cas9/1103* deletion mutants at a multiplicity of infection (MOI) of 20:1 (bacteria per macrophage). At 5.5 hours post infection, cells were assayed for cytotoxicity using the LDH release assay (n=3). (B) Identical infections as above were

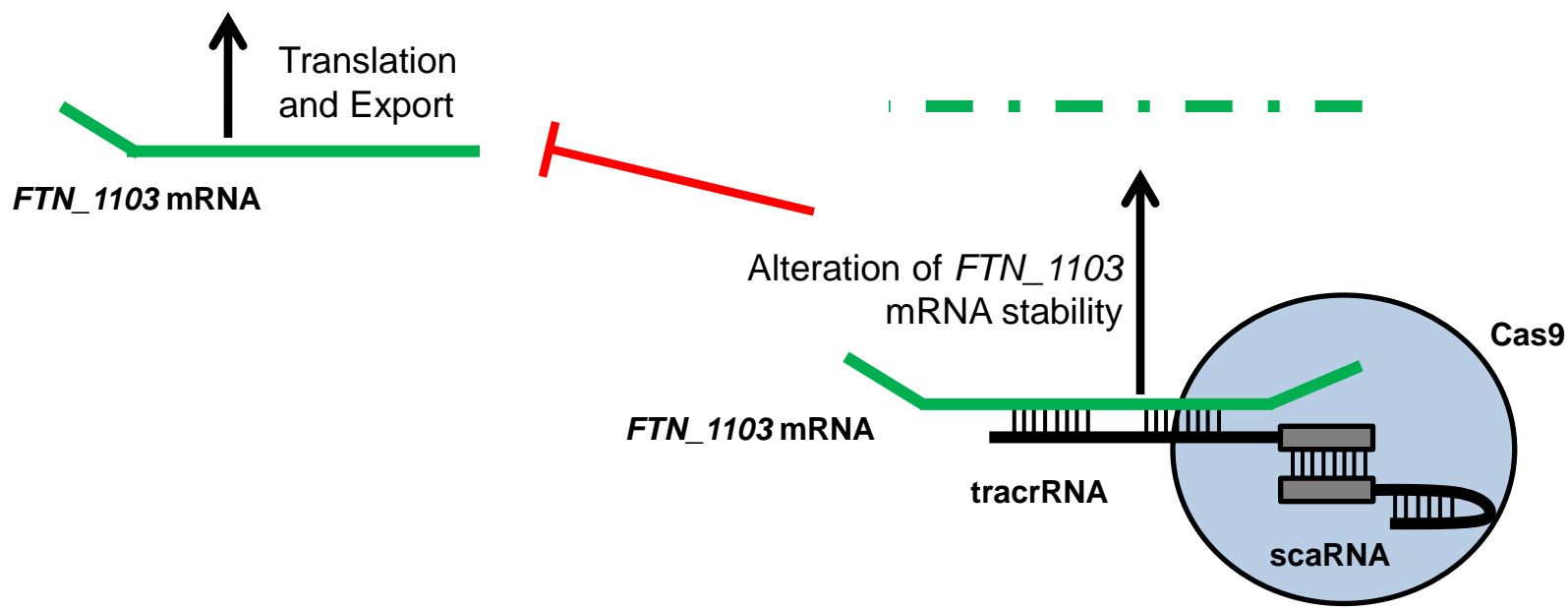
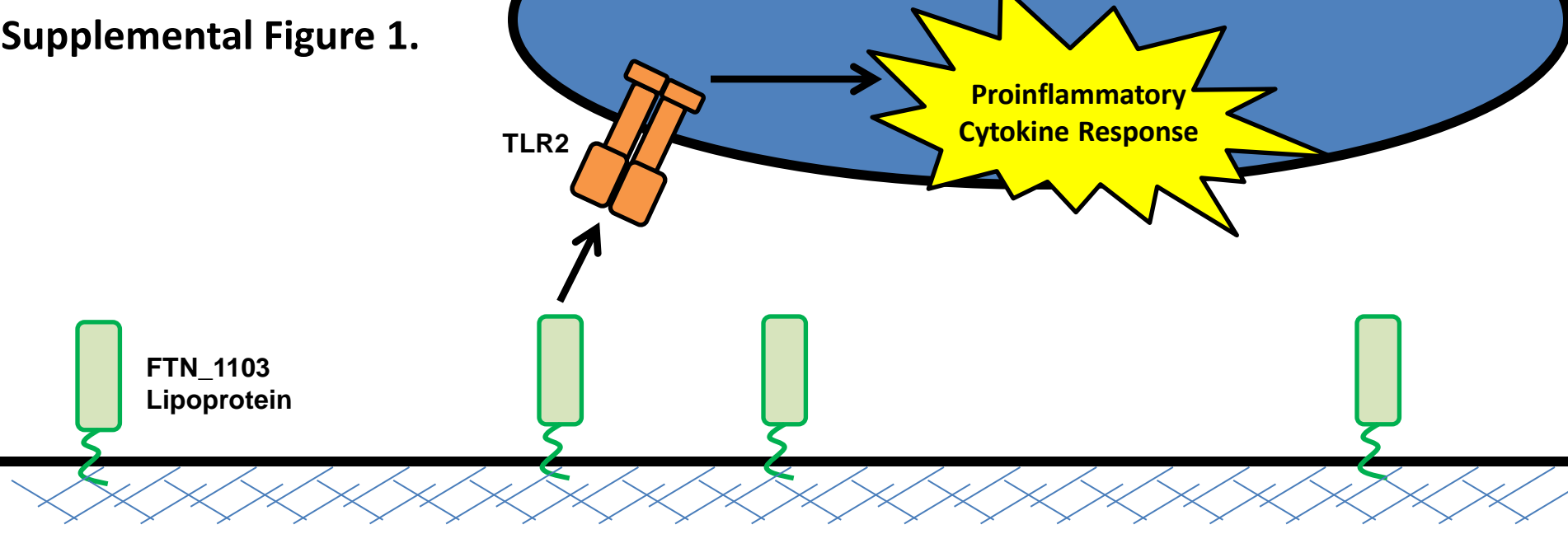
performed and at 4 hours post infection, infection supernatants collected, and ELISA performed for the pro-inflammatory cytokine IL-6 (n=3). *; $p \leq 0.05$, **; $p \leq 0.005$.

Supplemental Figure 23. *Campylobacter jejuni* Cas9 controls envelope permeability and erythromycin resistance. (A) Cultures of wild-type GB11 (WT) and the *cas9* deletion mutant were washed, stained with ethidium bromide, and fluorescence measured (n=4). (B) MIC breakpoints as determined by erythromycin E-test for WT or the *cas9* deletion mutant. ***; $p \leq 0.001$.

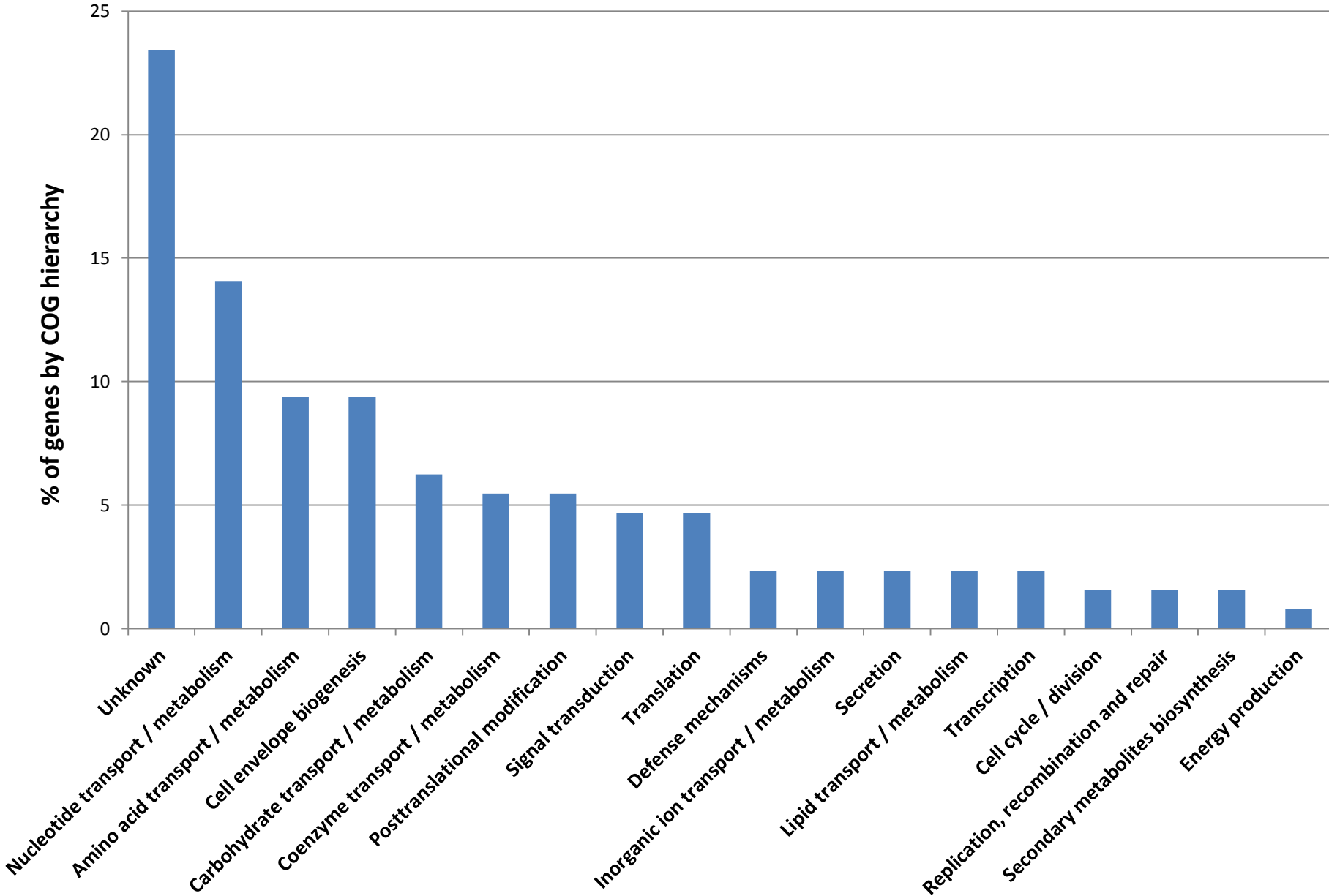
Supplemental References

1. Llewellyn AC, Jones CL, Napier BA, Bina JE, & Weiss DS (2011) Macrophage replication screen identifies a novel Francisella hydroperoxide resistance protein involved in virulence. (Translated from eng) *PLoS One* 6(9):e24201 (in eng).
2. Llewellyn AC, *et al.* (2012) NaxD is a deacetylase required for lipid A modification and Francisella pathogenesis. (Translated from eng) *Mol Microbiol* 86(3):611-627 (in eng).
3. Kanistanon D, *et al.* (2008) A Francisella mutant in lipid A carbohydrate modification elicits protective immunity. (Translated from eng) *PLoS Pathog* 4(2):e24 (in eng).
4. Wang X, Karbarz MJ, McGrath SC, Cotter RJ, & Raetz CR (2004) MsbA transporter-dependent lipid A 1-dephosphorylation on the periplasmic surface of the inner membrane: topography of Francisella novicida LpxE expressed in Escherichia coli. (Translated from eng) *J Biol Chem* 279(47):49470-49478 (in eng).
5. Raynaud C, *et al.* (2007) Role of the wbt locus of Francisella tularensis in lipopolysaccharide O-antigen biogenesis and pathogenicity. (Translated from eng) *Infect Immun* 75(1):536-541 (in eng).
6. Gallagher LA, *et al.* (2007) A comprehensive transposon mutant library of Francisella novicida, a bioweapon surrogate. (Translated from eng) *Proc Natl Acad Sci U S A* 104(3):1009-1014 (in eng).
7. Louwen R, *et al.* (2013) A novel link between Campylobacter jejuni bacteriophage defence, virulence and Guillain-Barre syndrome. (Translated from Eng) *Eur J Clin Microbiol Infect Dis* 32(2):207-226 (in Eng).

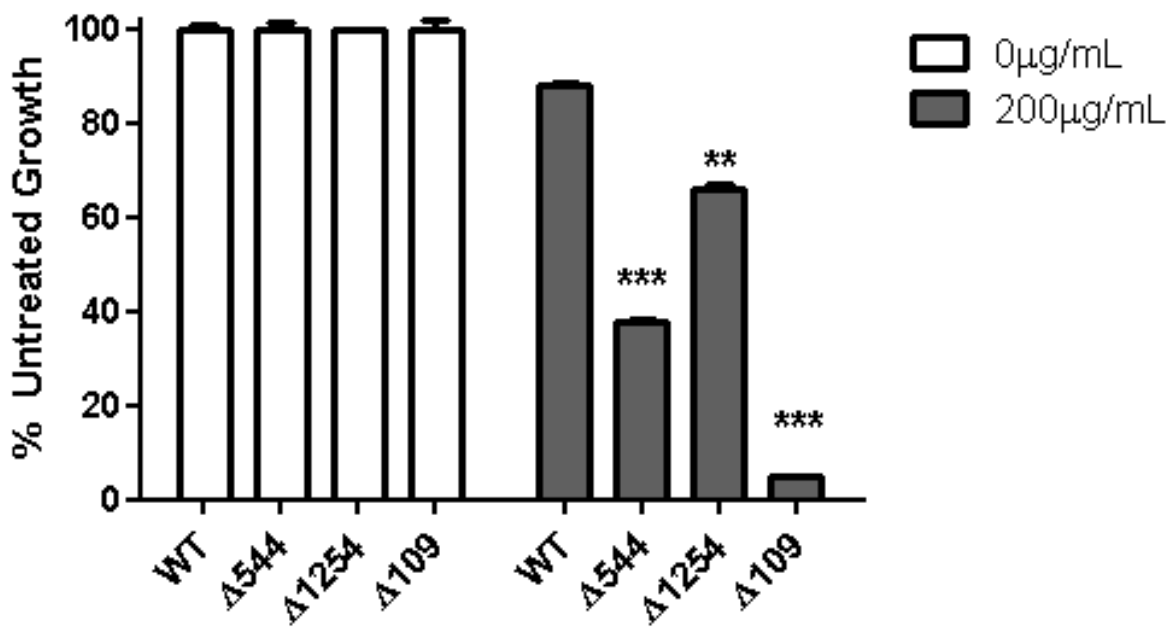
Supplemental Figure 1.



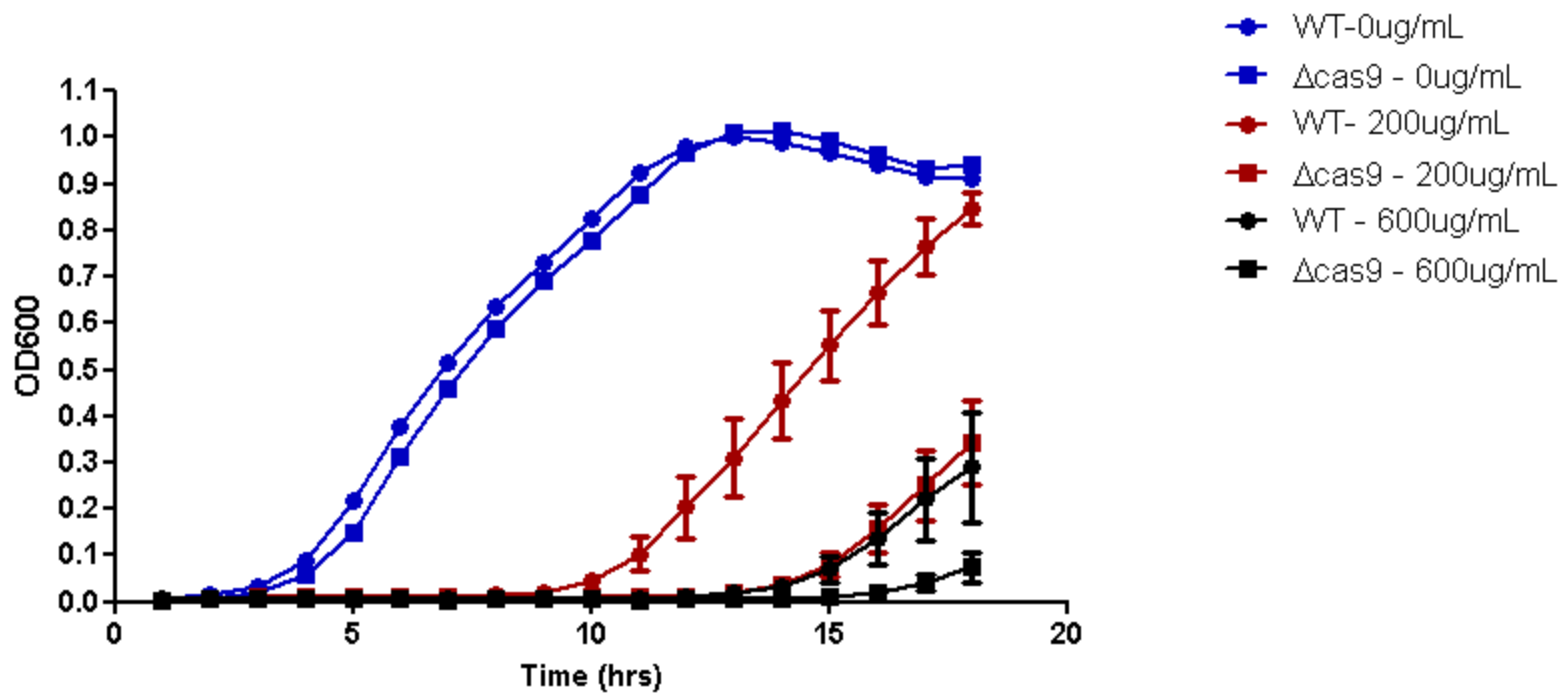
Supplemental Figure 2.



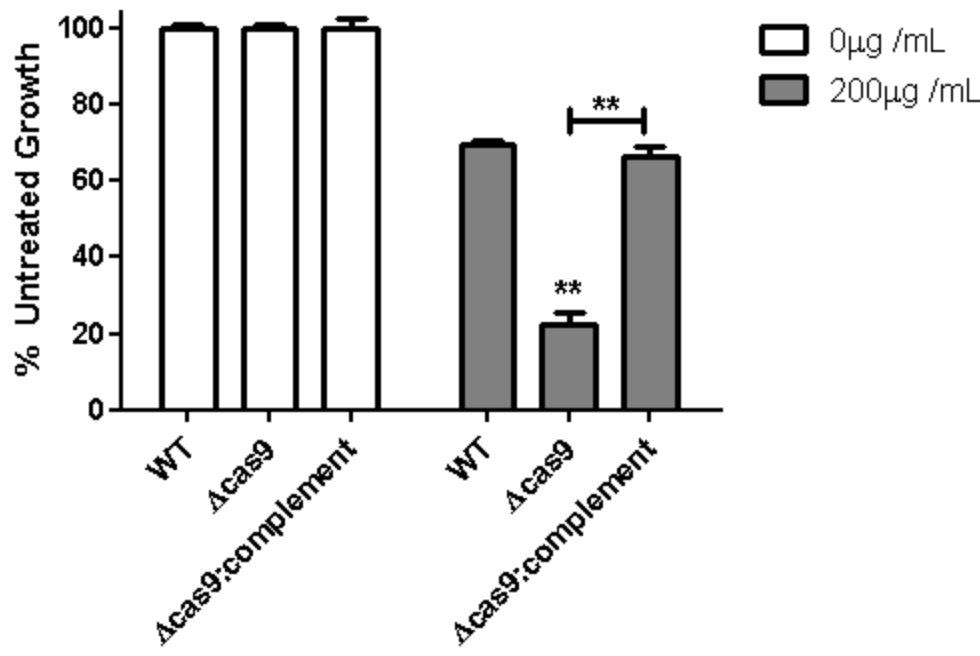
Supplemental Figure 3.



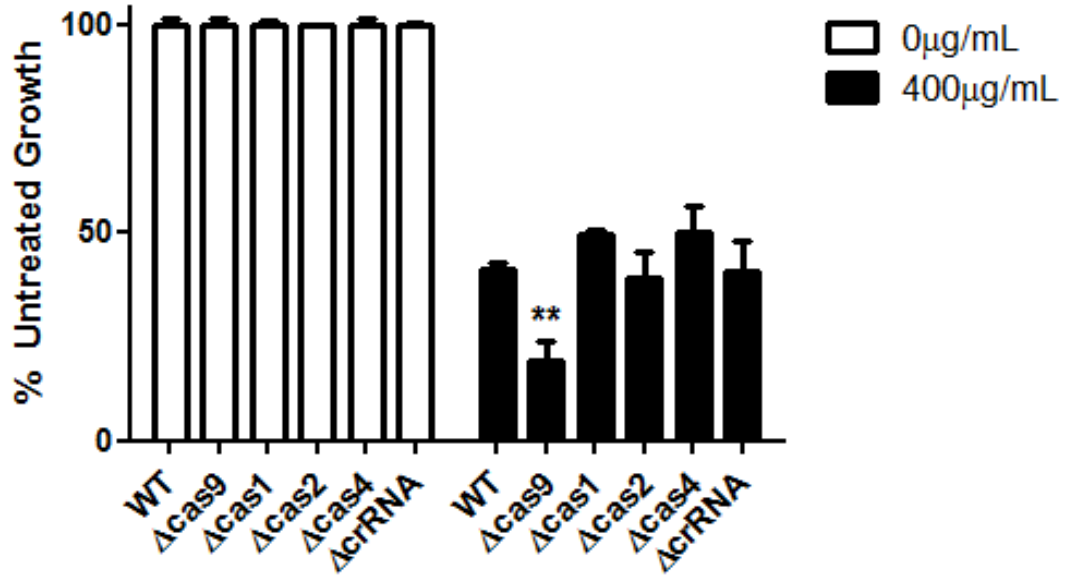
Supplemental Figure 4.



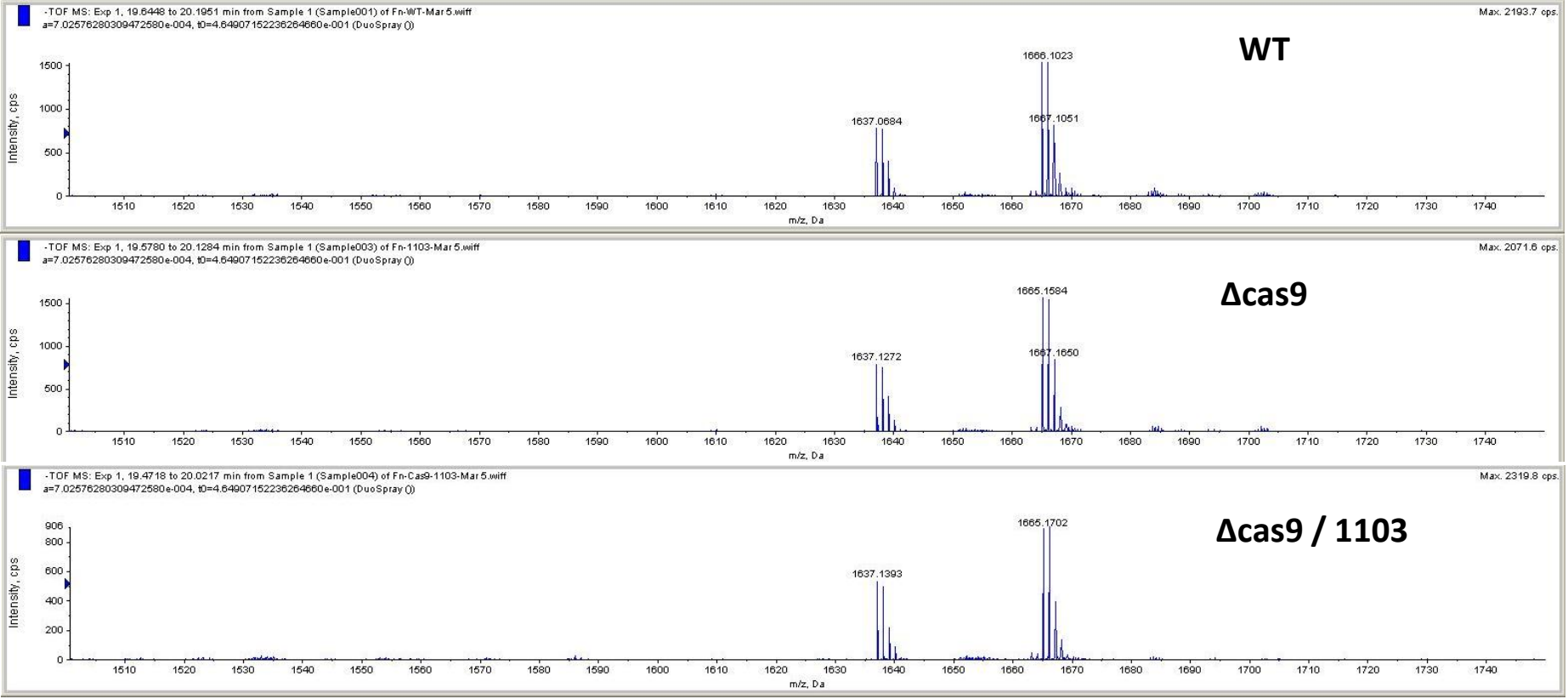
Supplemental Figure 5.



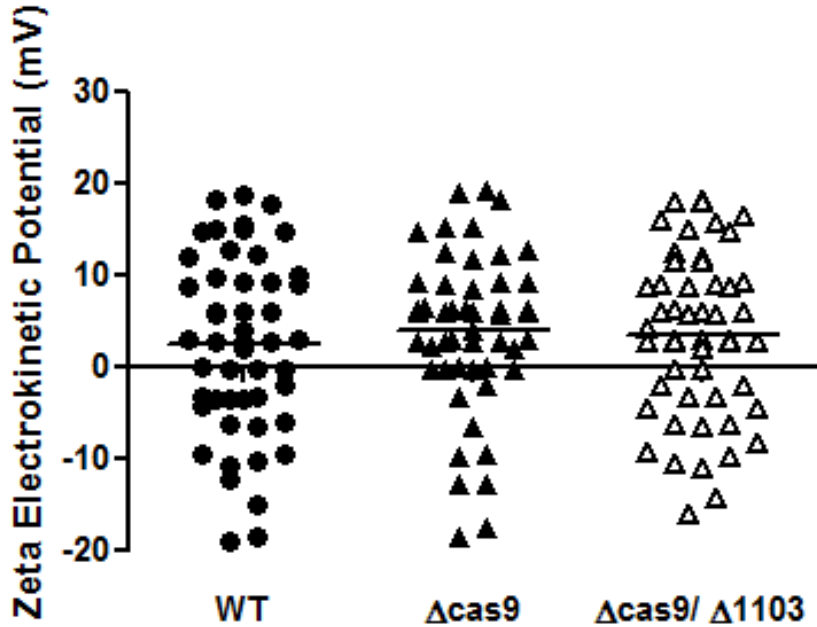
Supplemental Figure 6.



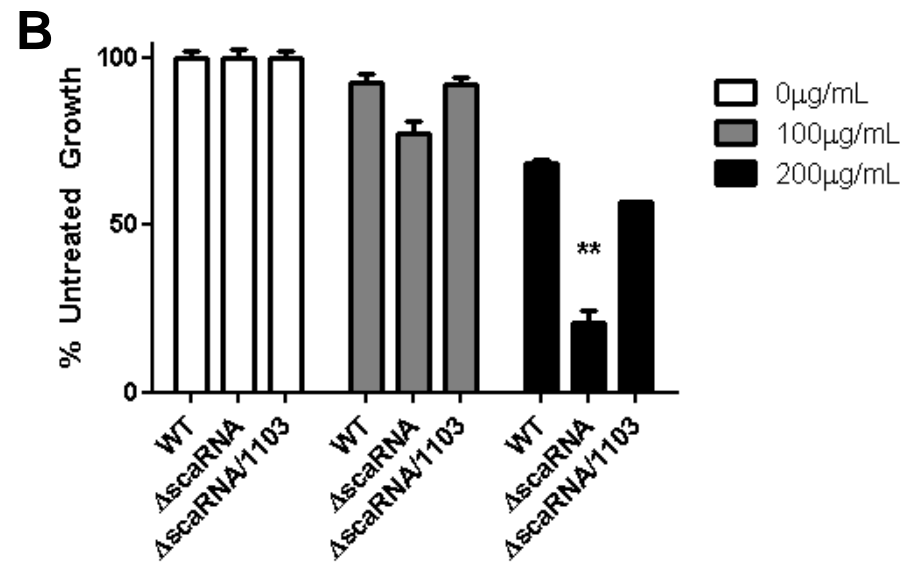
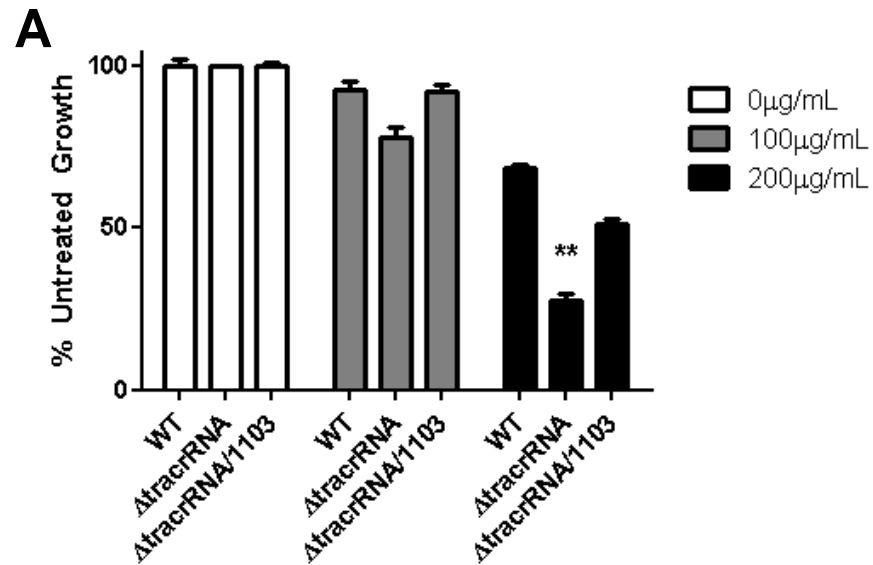
Supplemental Figure 7.



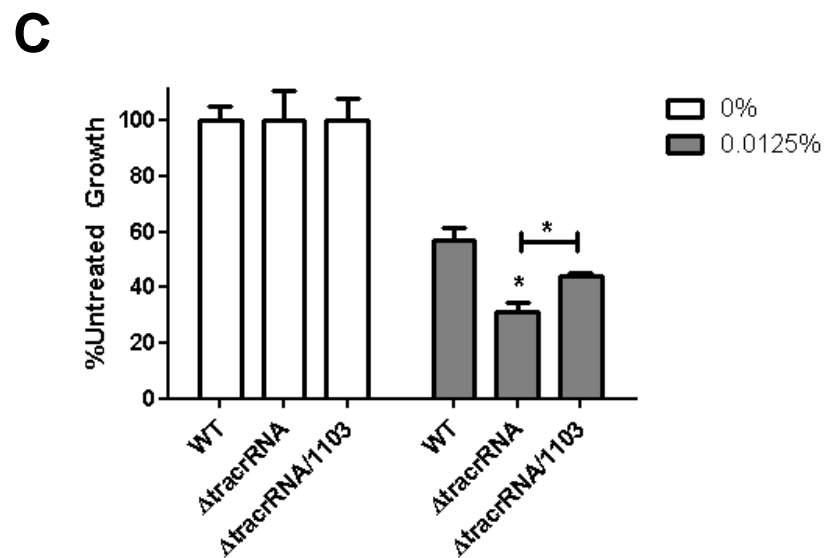
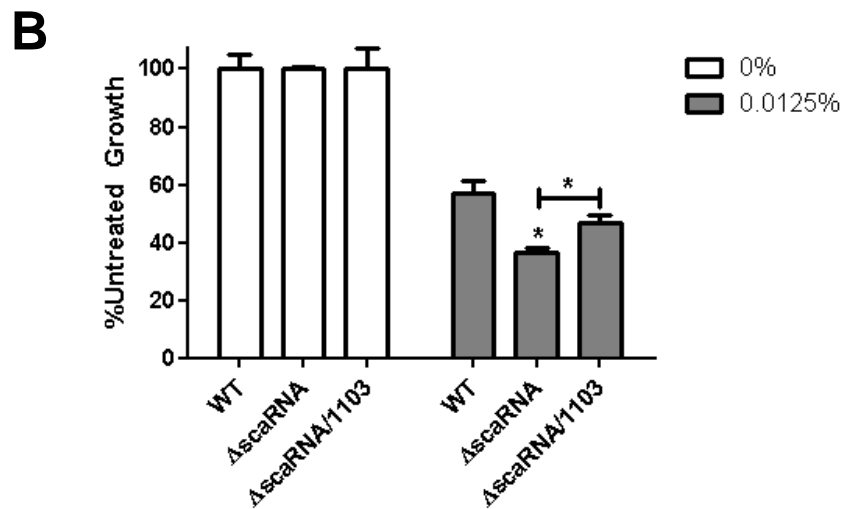
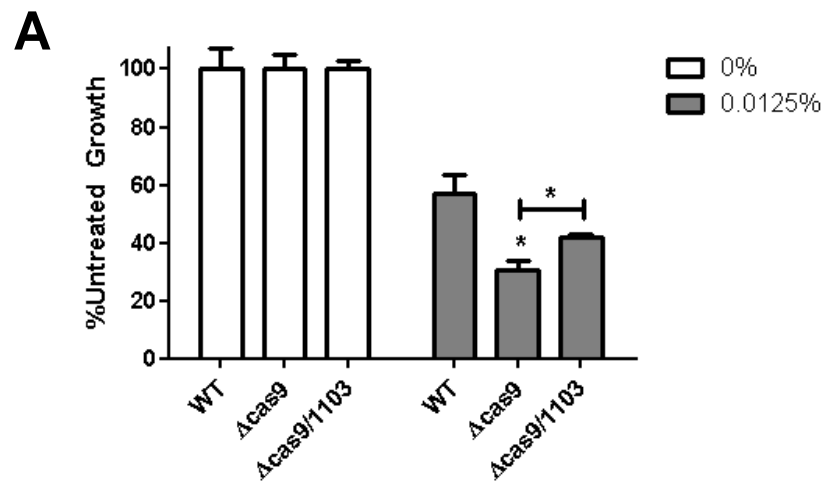
Supplemental Figure 8.



Supplemental Figure 9.

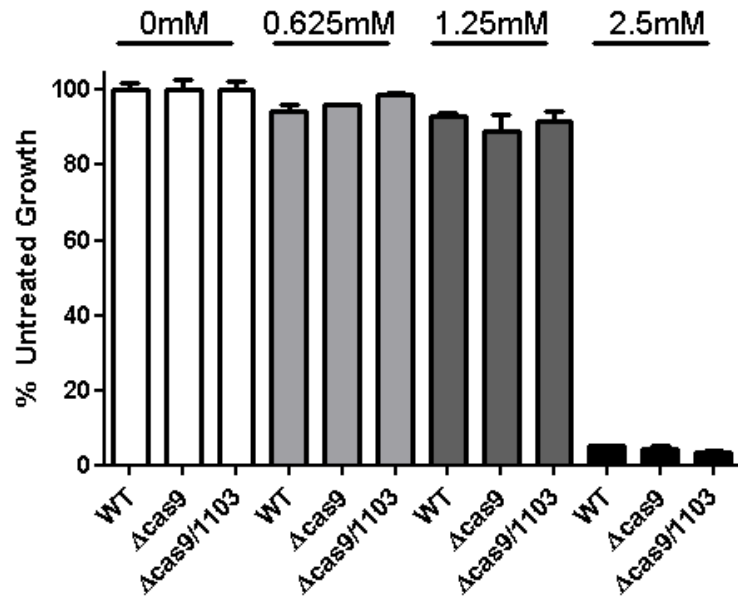


Supplemental Figure 10.

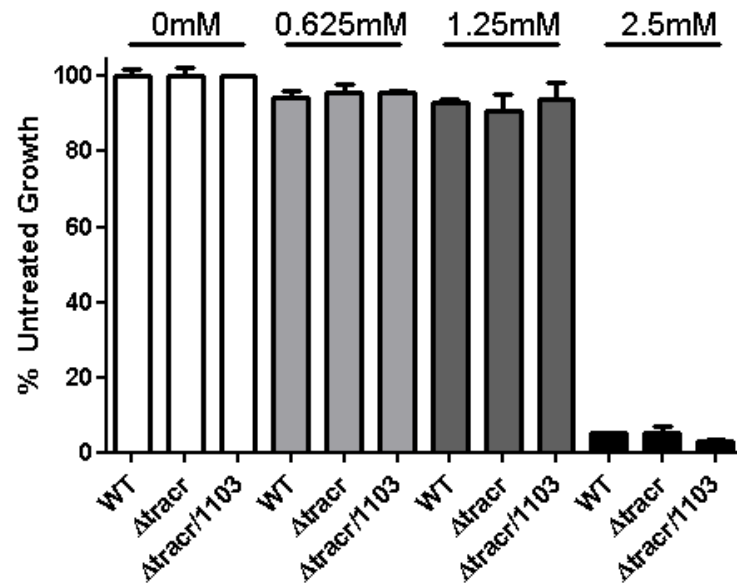


Supplemental Figure 11.

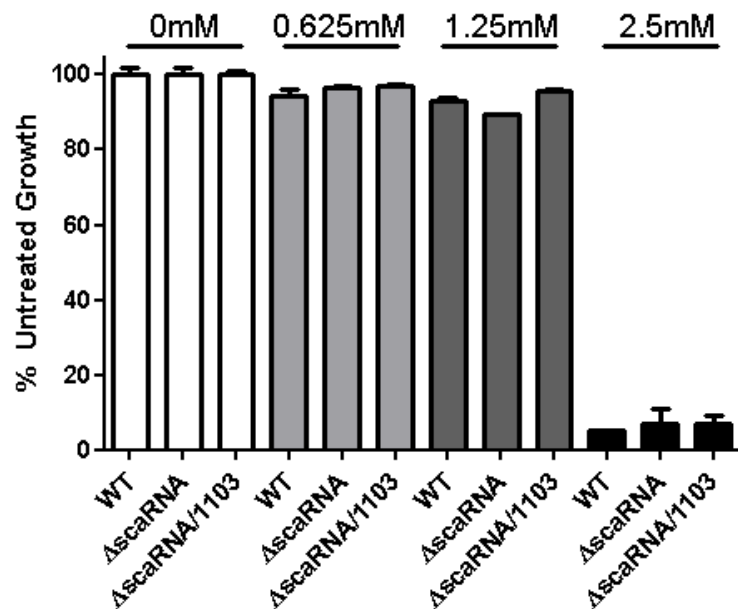
A



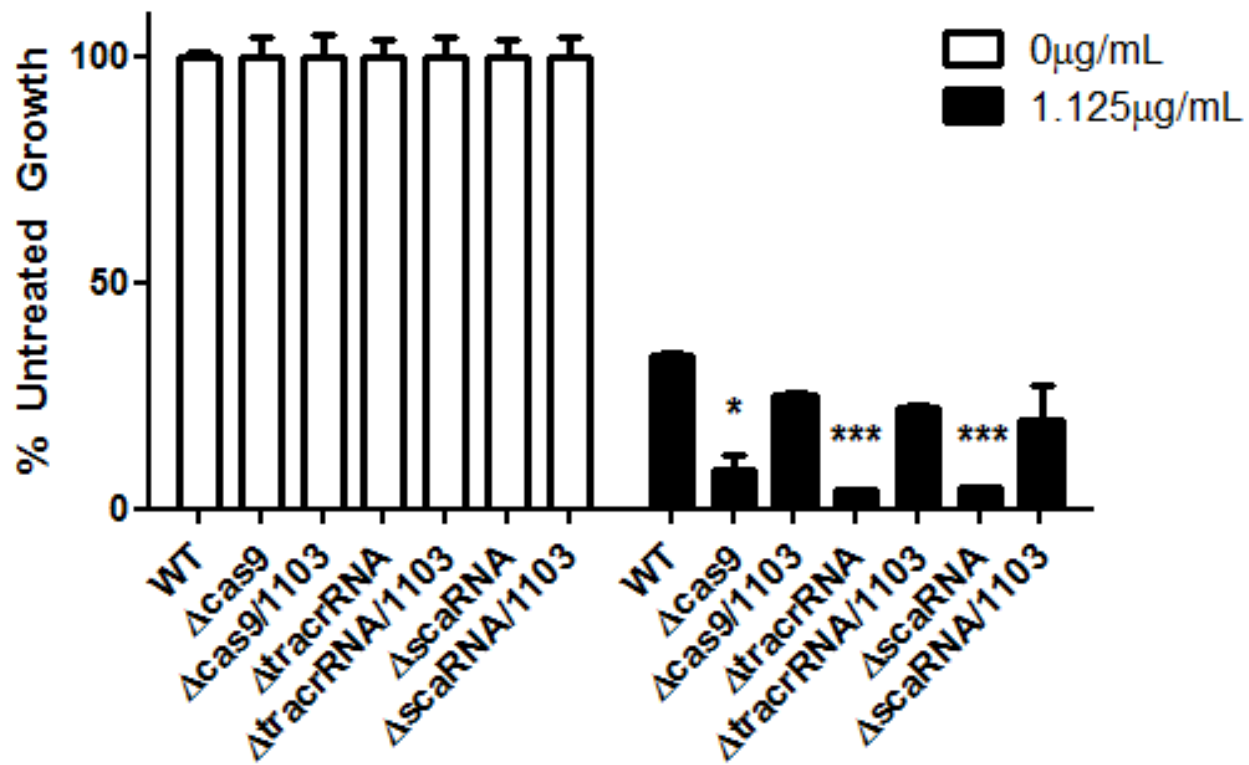
B



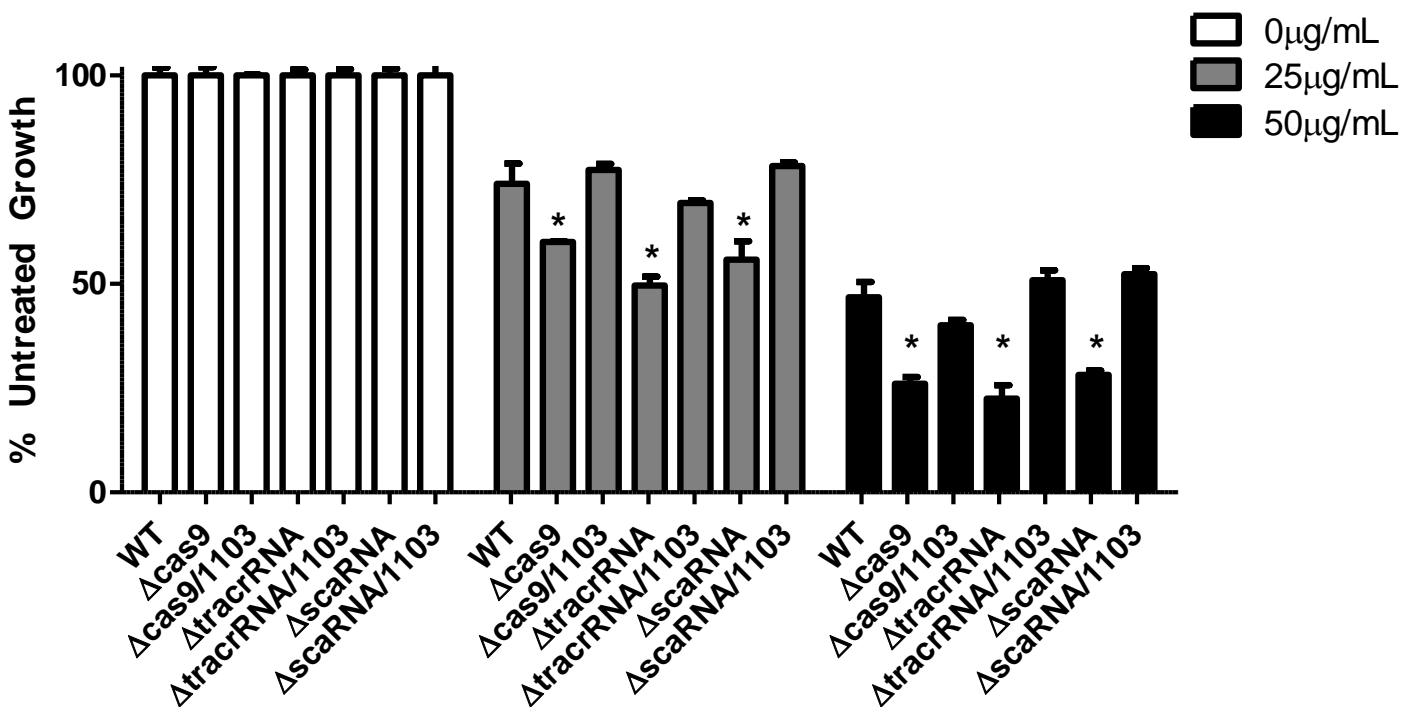
C



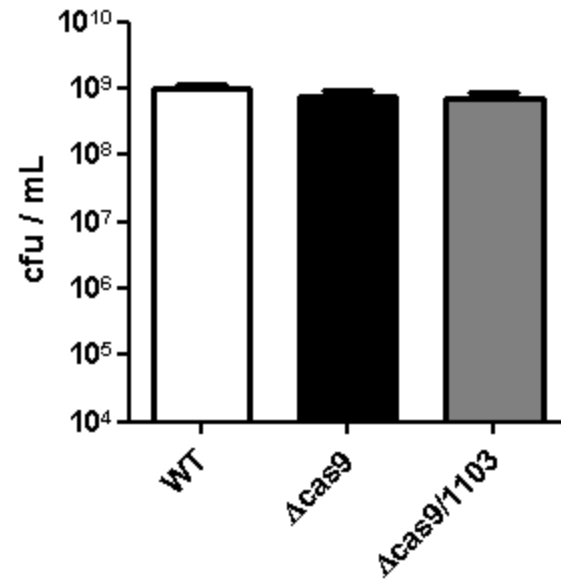
Supplemental Figure 12.



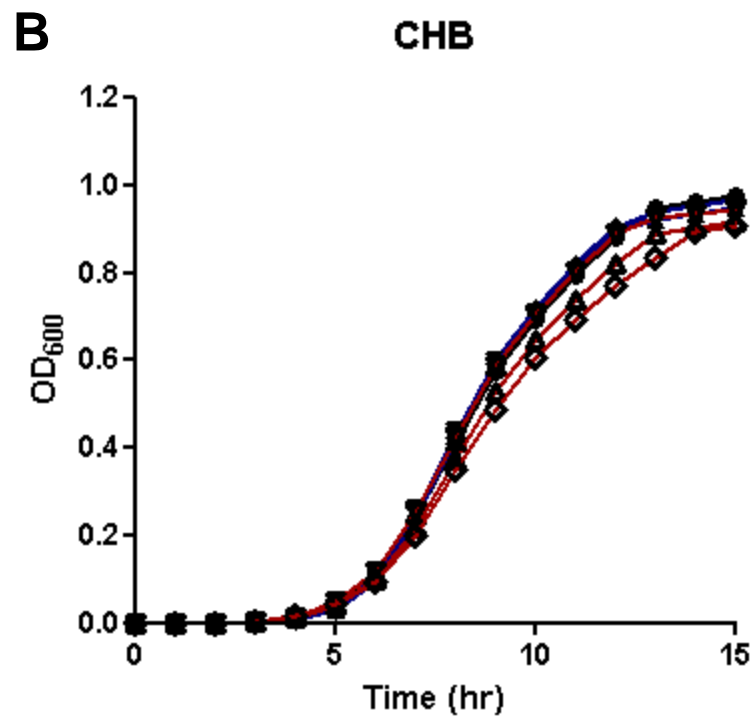
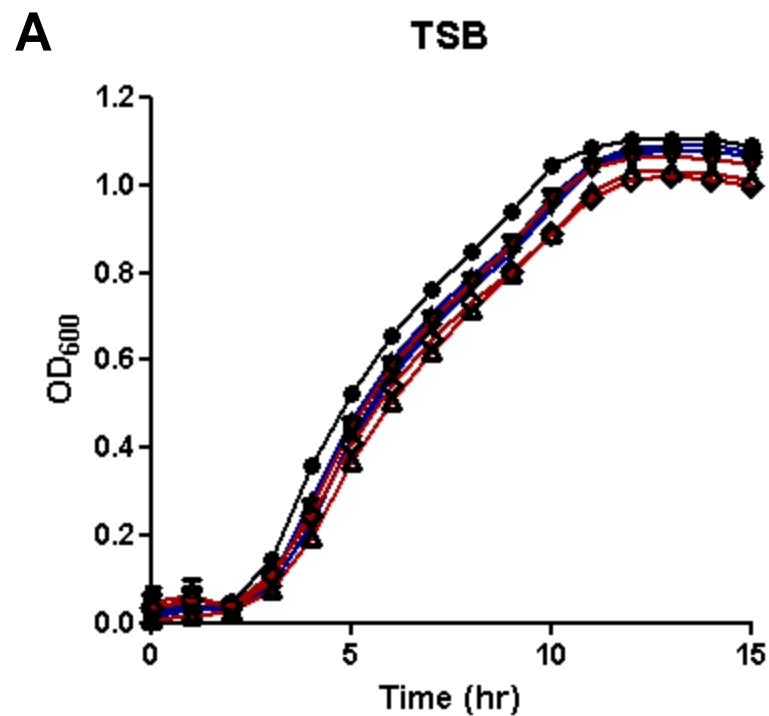
Supplemental Figure 13.



Supplemental Figure 14.

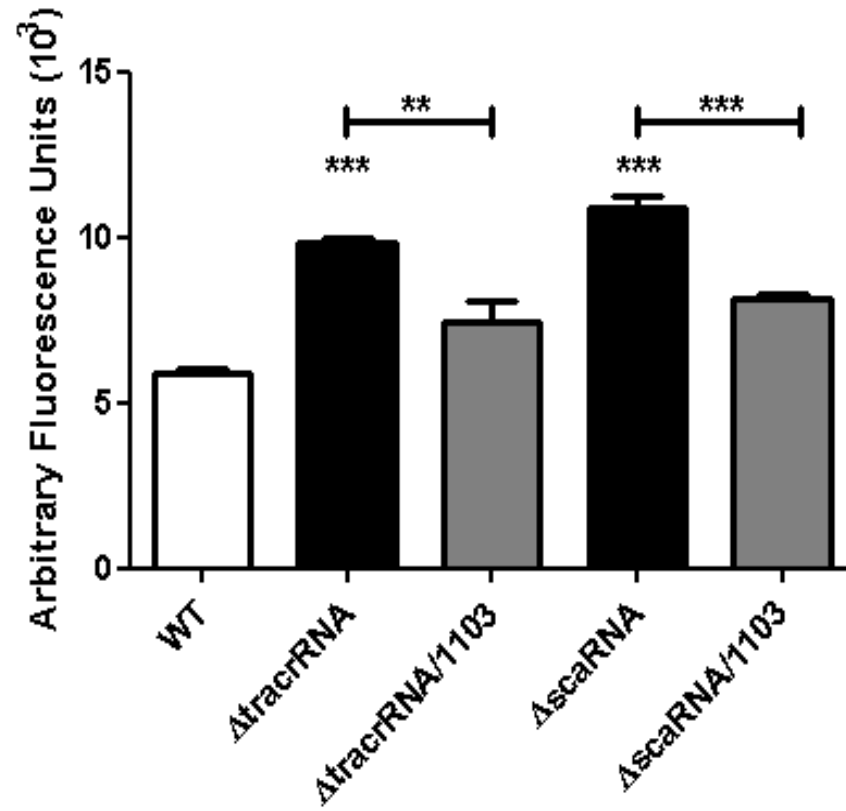


Supplemental Figure 15.

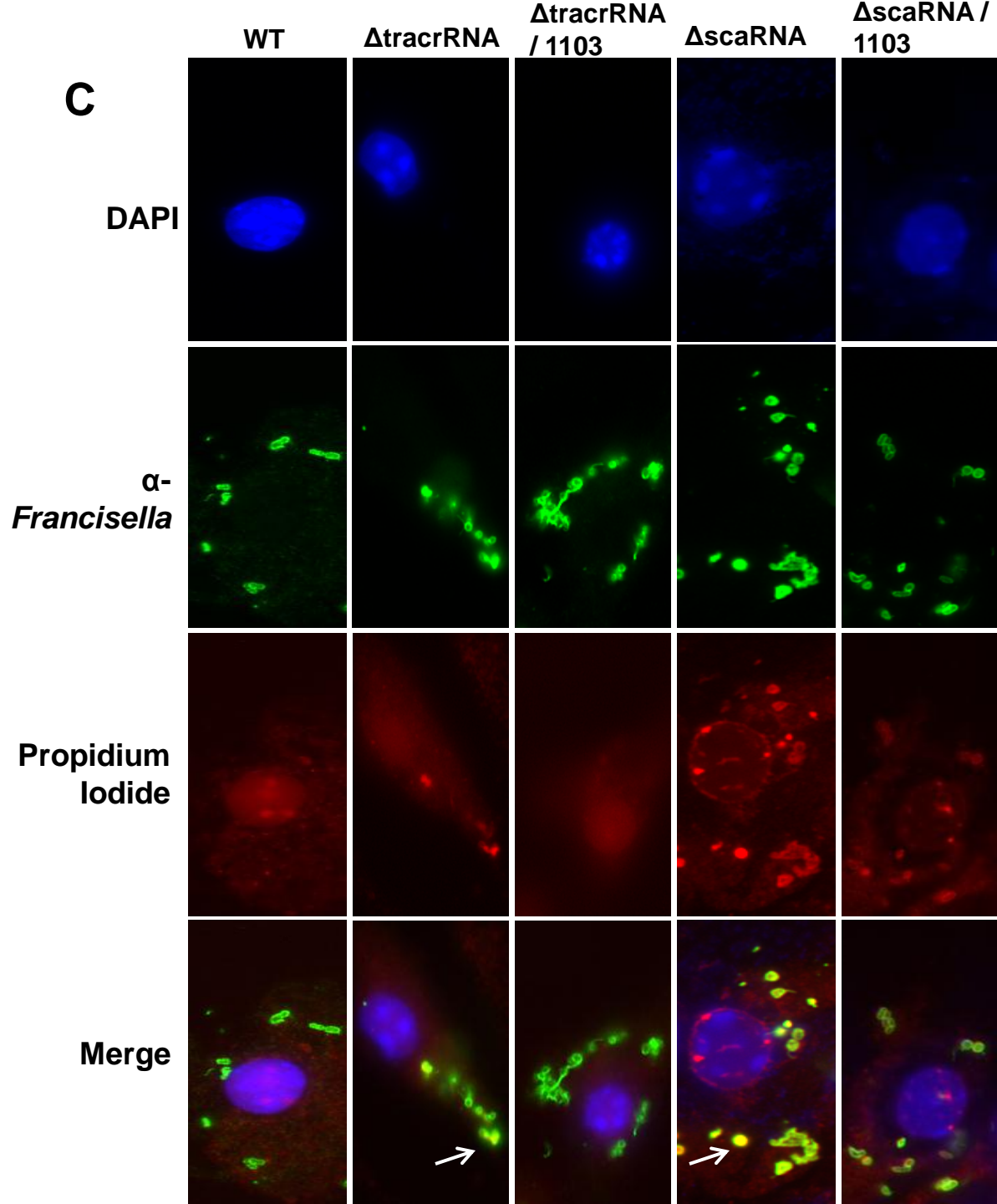
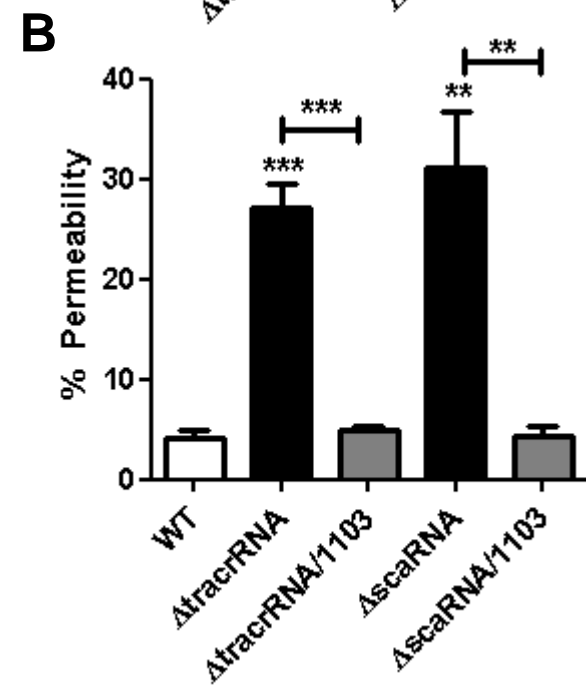
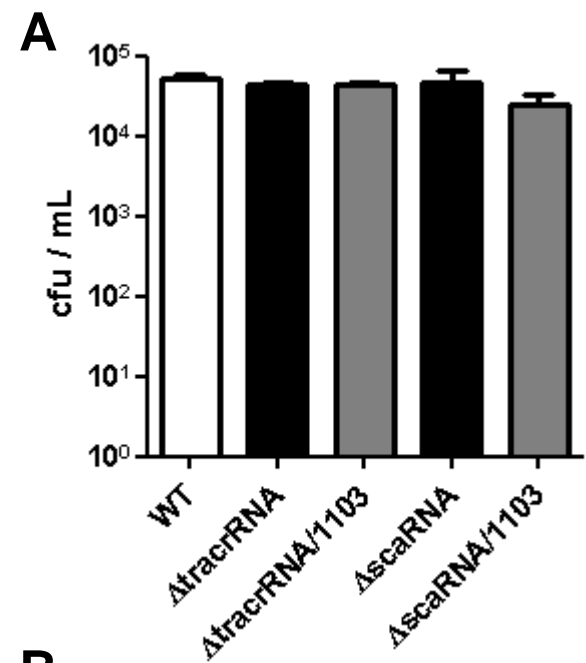


- WT
- ▲ Δ cas9
- ▼ Δ tracrRNA
- ◆ Δ scaRNA
- ▲ Δ cas9/1103
- ▼ Δ tracrRNA/1103
- ◆ Δ scaRNA/1103

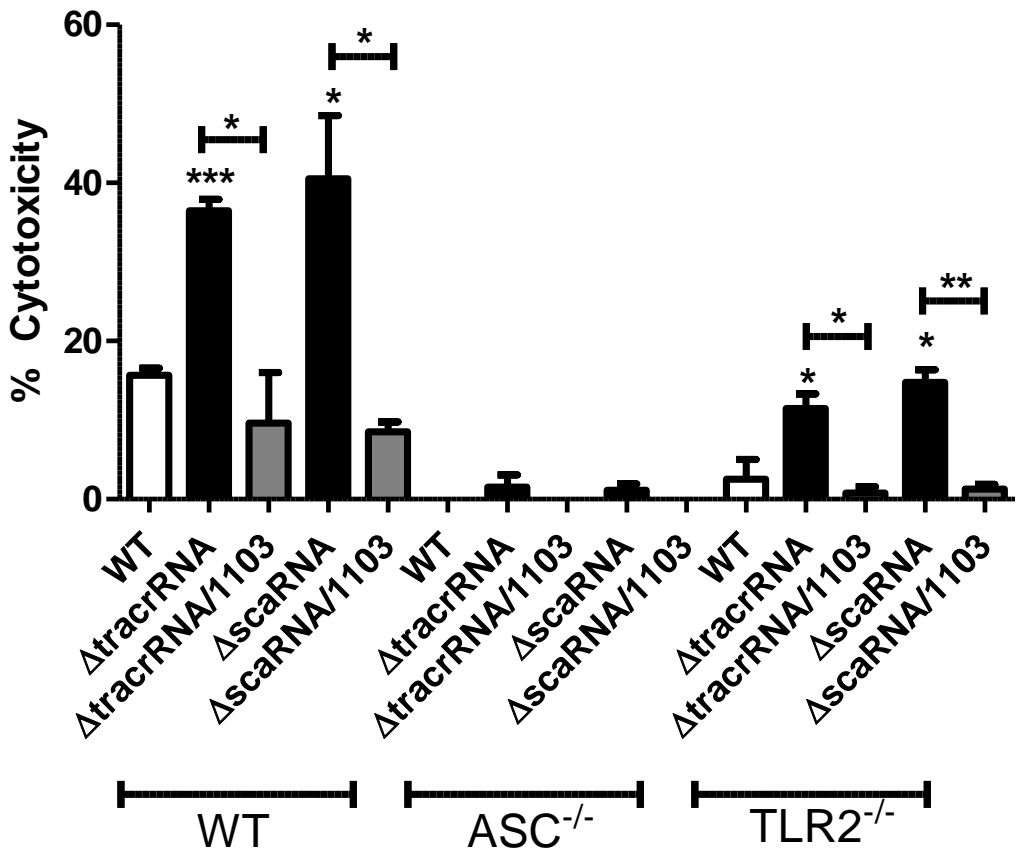
Supplemental Figure 16.



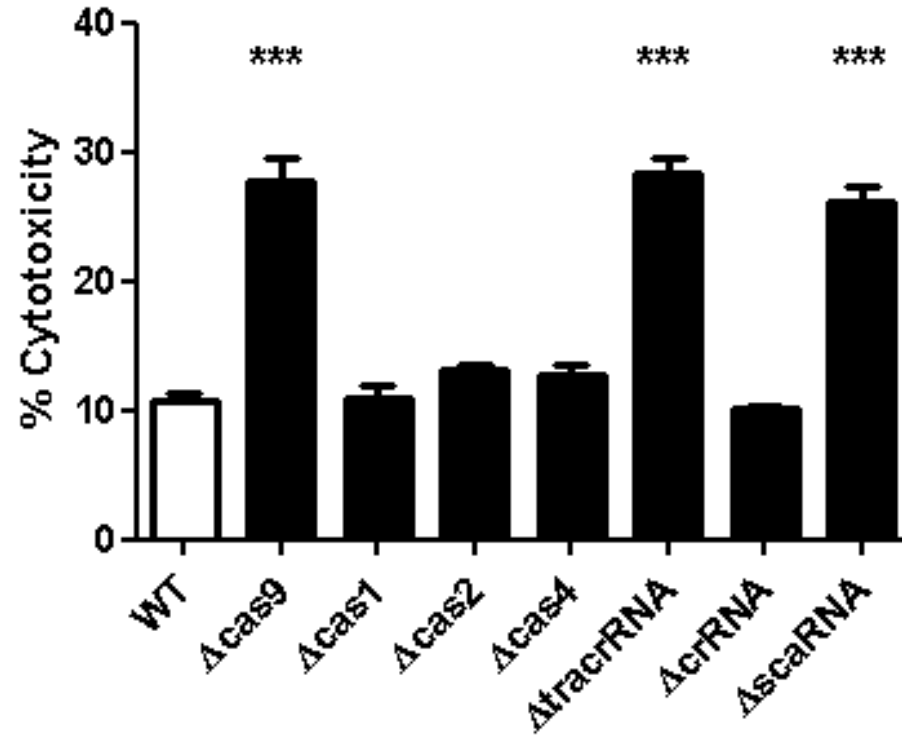
Supplemental Figure 17.



Supplemental Figure 18.

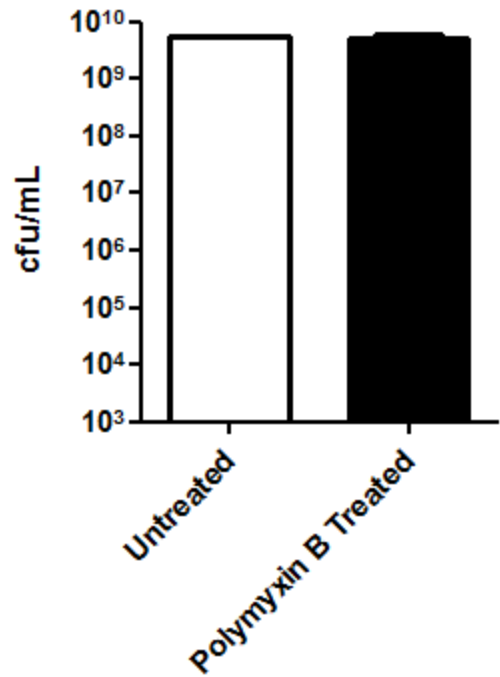


Supplemental Figure 19.

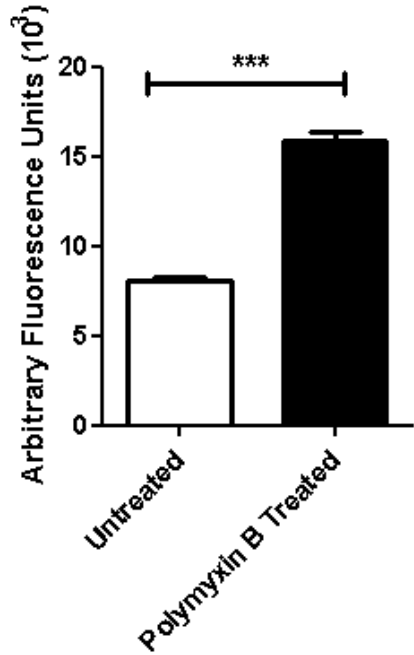


Supplemental Figure 20.

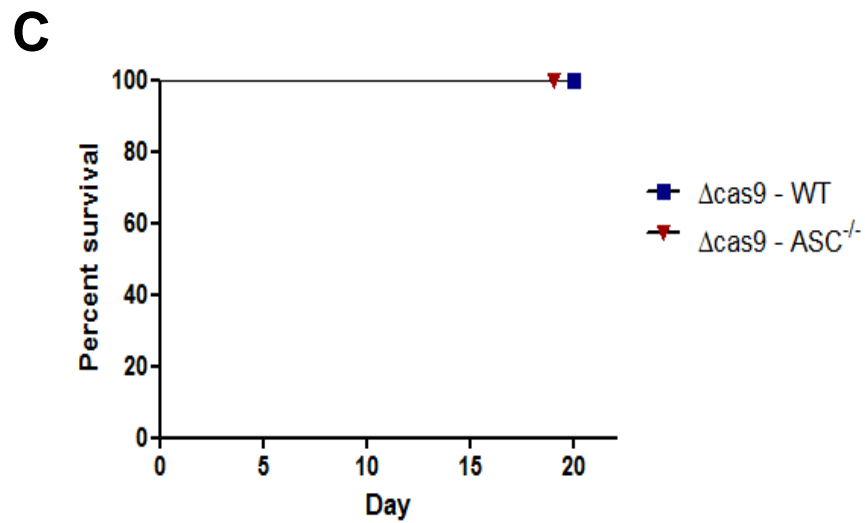
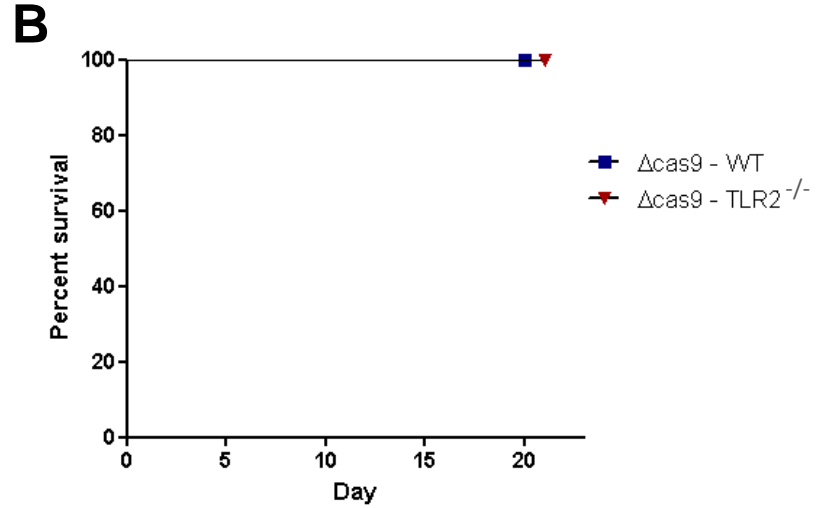
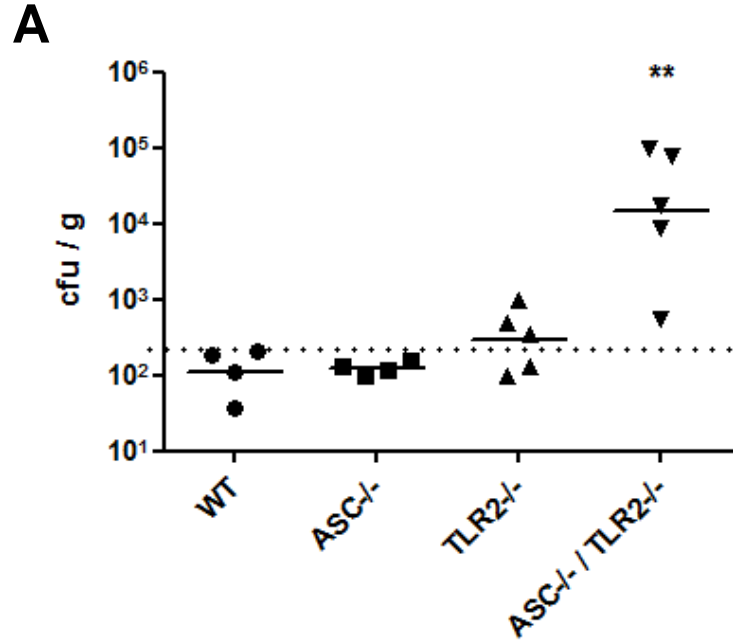
A



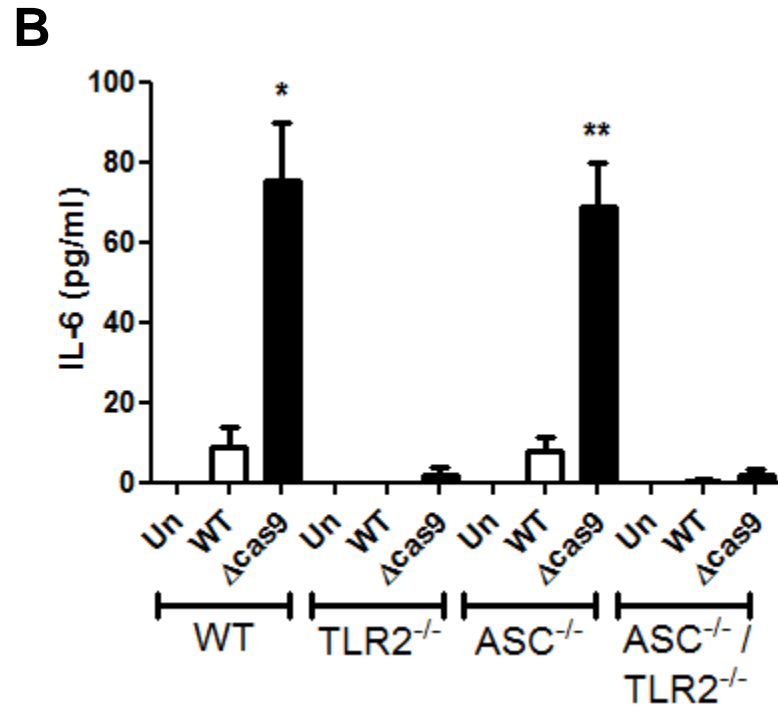
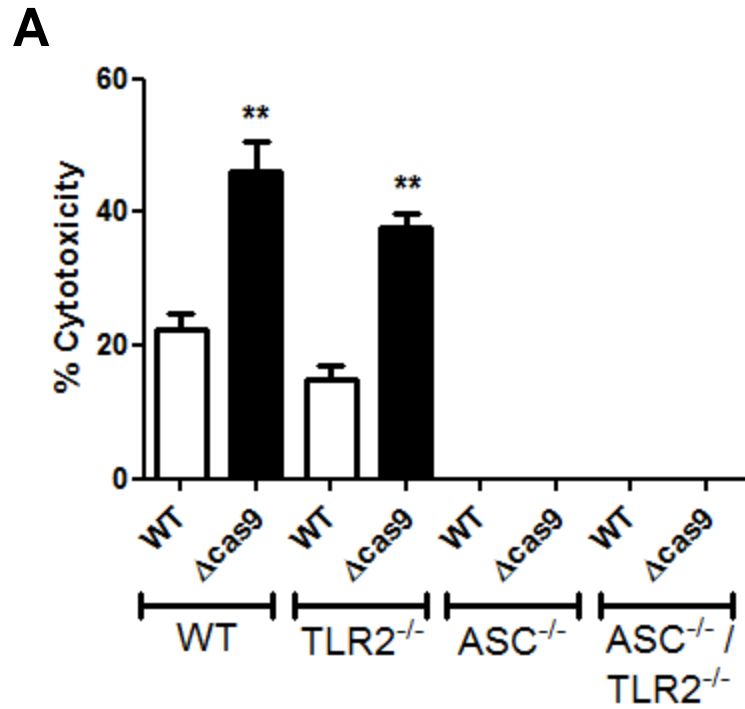
B



Supplemental Figure 21.

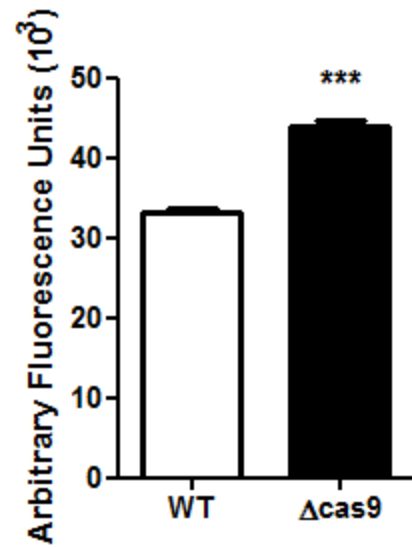


Supplemental Figure 22.

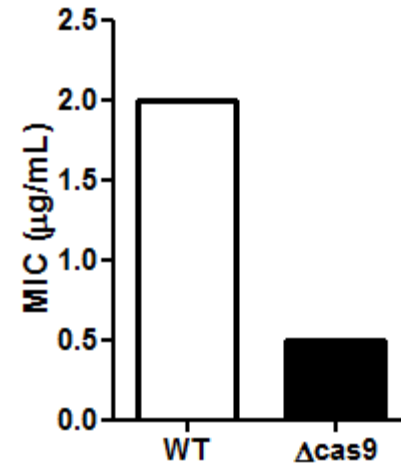


Supplemental Figure 23.

A



B



Supplemental Table 1. Transposon mutants with increased sensitivity to polymyxin B

<u>Locus</u>	<u>Name</u>	<u>COG</u>	<u>Description</u>	<u>% WT Growth in Polymyxin</u>
FTN_0019	<i>pyrB</i>	COG0540F	aspartate carbamoyltransferase	68.9
FTN_0021	<i>carA</i>	COG0505EF	carbamoyl phosphate synthase small subunit	62.4
FTN_0036	<i>pyrD</i>	COG0167F	dihydroorotate oxidase	68.7
FTN_0097	-	COG0814E	hydroxy/aromatic amino acid permease (HAAAP) family protein	73.0
FTN_0098	<i>gidB</i>	COG0357M	16S rRNA methyltransferase GidB	69.0
FTN_0109	-	-	hypothetical protein FTN_0109	0.2
FTN_0113	<i>ribC</i>	COG0307H	riboflavin synthase subunit alpha	0.0
FTN_0132	-	-	hypothetical protein FTN_0132	63.9
FTN_0177	<i>purH</i>	COG0138F	bifunctional phosphoribosylaminoimidazolecarboxamide formyltransferase/IMP cyclohydrolase	70.1
FTN_0178	<i>purA</i>	COG0104F	adenylosuccinate synthetase	57.0
FTN_0196	<i>cyoB</i>	COG0843C	cytochrome bo terminal oxidase subunit I	73.4
FTN_0197	<i>cyoC</i>	COG1845C	cytochrome bo terminal oxidase subunit III	65.7
FTN_0202	<i>pdxY</i>	COG2240H	pyridoxal kinase	68.1
FTN_0296	<i>lysP</i>	COG0833E	lysine:H ⁺ symporter	28.5
FTN_0298	<i>glpX</i>	COG1494G	fructose 1,6-bisphosphatase II	68.5
FTN_0300	-	COG1215M	glycosyl transferase	63.5
FTN_0325	-	COG2854Q	membrane protein	71.9
FTN_0330	<i>minD</i>	COG2894D	septum site-determining protein MinD	71.0
FTN_0331	<i>minC</i>	COG0850D	septum site-determining protein MinC	64.9

FTN_0358	<i>rimO</i>	COG0621J	ribosomal protein S12 methylthiotransferase	73.7
FTN_0416	<i>lpxE</i>	COG0671I	lipid A 1-phosphatase	52.6
FTN_0417	<i>folD</i>	COG0190H	bifunctional 5,10-methylene-tetrahydrofolate dehydrogenase/ 5,10-methylene-tetrahydrofolate cyclohyd...	29.6
FTN_0419	<i>purM</i>	COG0150F	phosphoribosylaminoimidazole synthetase	72.6
FTN_0421	<i>purN</i>	COG0299F	phosphoribosylglycinamide formyltransferase	70.8
FTN_0422	<i>purE</i>	COG0041F	N5-carboxyaminoimidazole ribonucleotide mutase	69.0
FTN_0427	-	-	hypothetical protein FTN_0427	60.6
FTN_0434	<i>parB</i>	COG1475K	chromosome partition protein B	68.8
FTN_0436	-	COG3240IR	hypothetical protein FTN_0436	68.4
FTN_0444	-	-	membrane protein	48.1
FTN_0494	-	-	hypothetical protein FTN_0494	62.6
FTN_0495	-	COG4692G	BNR/Asp-box repeat-containing protein	67.0
FTN_0507	<i>gcvP1</i>	COG0403E	glycine dehydrogenase subunit 1	72.2
FTN_0514	<i>pgm</i>	COG0033G	phosphoglucomutase	61.9
FTN_0515	<i>glgC</i>	COG0448G	glucose-1-phosphate adenylyltransferase	55.6
FTN_0534	-	COG1289S	hypothetical protein FTN_0534	74.4
FTN_0544	<i>naxD</i>	COG3394S	N-acetylhexosamine deacetylase	36.5
FTN_0545	-	COG0463M	glycosyl transferase	4.3
FTN_0546	-	COG1807M	dolichyl-phosphate-mannose-protein mannosyltransferase family protein	1.0
FTN_0554	-	COG0219J	RNA methyltransferase	57.3
FTN_0561	<i>apaH</i>	COG0639T	diadenosine tetraphosphatase	53.7

FTN_0593	<i>sucD</i>	COG0074C	succinyl-CoA synthetase, alpha subunit	72.0
FTN_0594	<i>sucC</i>	COG0045C	succinyl-CoA synthetase subunit beta	63.5
FTN_0599	-	-	hypothetical protein FTN_0599	55.6
FTN_0624	-	COG0814E	serine permease	74.0
FTN_0651	<i>cdd</i>	COG0295F	cytidine deaminase	69.0
FTN_0669	<i>deoD</i>	COG0813F	purine nucleoside phosphorylase	65.0
FTN_0672	<i>secA</i>	COG0653U	preprotein translocase subunit SecA	66.8
FTN_0690	<i>deaD</i>	COG0513LKJ	DEAD/DEAH box helicase	73.3
FTN_0719	-	-	hypothetical protein FTN_0719	60.9
FTN_0728	-	COG0053P	Co/Zn/Cd cation transporter	73.4
FTN_0757	<i>cas9</i>	-	CRISPR/Cas associated protein	69.9
FTN_0772	-	COG0545O	hypothetical protein FTN_0772	72.5
FTN_0806	-	COG1472G	glycosyl hydrolase family protein	60.0
FTN_0814	<i>bioF</i>	COG0156H	8-amino-7-oxononanoate synthase	73.1
FTN_0815	<i>bioB</i>	COG0502H	biotin synthase	74.4
FTN_0816	<i>bioA</i>	COG0161H	adenosylmethionine-8-amino-7-oxononanoate aminotransferase	66.8
FTN_0842	<i>aroG</i>	COG0722E	phospho-2-dehydro-3-deoxyheptonate aldolase	68.3
FTN_0848	-	COG0531E	amino acid antiporter	65.0
FTN_0855	-	-	hypothetical protein FTN_0855	74.0
FTN_0945	<i>rsuA</i>	COG1187J	16S rRNA pseudouridine synthase	50.1
FTN_0998	-	COG2898S	potassium channel protein	69.0
FTN_0999	<i>udhA</i>	COG1249C	soluble pyridine nucleotide transhydrogenase	71.0

FTN_1016	-	COG1335Q	hypothetical protein FTN_1016	72.6
FTN_1055	<i>lon</i>	COG0466O	DNA-binding, ATP-dependent protease La	70.8
FTN_1056	<i>clpX</i>	COG1219O	ATP-dependent protease ATP-binding subunit ClpX	5.1
FTN_1057	<i>clpP</i>	COG0740OU	ATP-dependent Clp protease proteolytic subunit	64.1
FTN_1058	<i>tig</i>	COG0544O	trigger factor	74.0
FTN_1064	-	COG1702T	PhoH family protein ATPase	72.5
FTN_1066	-	COG4535P	HlyC/CorC family transporter-associated protein	68.2
FTN_1091	<i>aroA</i>	COG0128E	3-phosphoshikimate 1-carboxyvinyltransferase	59.4
FTN_1107	<i>metIQ</i>	COG1464P	methionine uptake transporter (MUT) family protein, membrane and periplasmic protein	69.7
FTN_1111	-	COG0769M	Mur ligase family protein	64.3
FTN_1133	-	-	Ohr-like protein	72.3
FTN_1146	-	COG0436E	aspartate aminotransferase	68.2
FTN_1199	-	-	hypothetical protein FTN_1199	70.9
FTN_1201	<i>capB</i>	COG0769M	capsule biosynthesis protein CapB	70.7
FTN_1211	-	COG1011R	haloacid dehalogenase-like hydrolase	74.2
FTN_1212	-	COG0438M	glycosyl transferases group 1 family protein	73.3
FTN_1213	-	COG1215M	glycosyl transferase family protein	65.5
FTN_1217	-	COG1132V	ABC transporter ATP-binding protein	74.0
FTN_1219	<i>galE</i>	COG1087M	UDP-glucose 4-epimerase	63.7
FTN_1240	-	COG0271T	hypothetical protein FTN_1240	50.7
FTN_1240	-	COG0271T	hypothetical protein FTN_1240	64.4

FTN_1254	-	-	hypothetical protein FTN_1254	64.7
FTN_1263	<i>comL</i>	COG4105R	competence lipoprotein ComL	73.0
FTN_1272	-	COG3104E	proton-dependent oligopeptide transporter (POT) family protein, di- or tripeptide:H+ symporter	68.0
FTN_1277	-	COG1538MU	outer membrane efflux protein	59.5
FTN_1311	-	-	hypothetical protein FTN_1311	67.0
FTN_1312	-	-	hypothetical protein FTN_1312	74.7
FTN_1313	-	-	hypothetical protein FTN_1313	52.5
FTN_1314	-	-	hypothetical protein FTN_1314	70.9
FTN_1315	-	-	hypothetical protein FTN_1315	71.8
FTN_1316	-	COG3455S	hypothetical protein FTN_1316	74.2
FTN_1317	-	-	hypothetical protein FTN_1317	70.2
FTN_1323	<i>iglB</i>	COG3517S	intracellular growth locus protein B	74.7
FTN_1421	<i>wbtH</i>	COG0367E	glutamine amidotransferase/asparagine synthase	72.5
FTN_1425	<i>wbtF</i>	COG0451MG	NAD dependent epimerase	67.8
FTN_1427	<i>wbtD</i>	COG0438M	group 1 glycosyl transferase	59.5
FTN_1470	<i>ispA</i>	COG0142H	geranyl diphosphate synthase/farnesyl diphosphate synthase	2.0
FTN_1471	<i>pcs</i>	COG1183I	phosphatidylcholine synthase	73.8
FTN_1500	-	-	hypothetical protein FTN_1500	66.5
FTN_1513	<i>xerC</i>	COG4973L	site-specific recombinase	73.6
FTN_1518	<i>relA</i>	COG0317TK	GDP pyrophosphokinase/GTP pyrophosphokinase	68.7
FTN_1538	<i>groEL</i>	COG0459O	chaperonin GroEL	71.5
FTN_1551	<i>ampD</i>	COG3023V	N-acetyl-anhydromuramyl-L-alanine amidase	57.8
FTN_1597	<i>prfC</i>	COG4108J	peptide chain release factor 3	57.0
FTN_1602	<i>deoB</i>	COG1015G	phosphopentomutase	74.5
FTN_1610	-	COG0841V	RND efflux transporter	74.4

FTN_1633	<i>apt</i>	COG0503F	adenine phosphoribosyltransferase	60.2
FTN_1653	-	-	hypothetical protein FTN_1653	74.7
FTN_1699	<i>purL</i>	COG0046F	phosphoribosylformylglycinamide synthase	66.0
FTN_1700	<i>purF</i>	COG0034F	amidophosphoribosyltransferase	73.8
FTN_1715	<i>kdpD</i>	COG2205T	two component regulator, sensor histidine kinase kdpD	61.7
FTN_1743	<i>clpB</i>	COG0542O	chaperone clpB	70.5
FTN_1745	<i>purT</i>	COG0027F	phosphoribosylglycinamide formyltransferase 2	72.2
FTN_1762	-	COG0488R	putative ABC transporter ATP-binding protein	68.5

Supplemental Table 2. Percent wild-type growth of each transposon mutant in polymyxin B

<u>Locus Tag</u>	<u>Gene name</u>	<u>COG</u>	<u>Gene product</u>	<u>% WT growth in polymyxin</u>	<u>Library Plate</u>	<u>Well</u>
FTN_0113	<i>ribC</i>	COG0307H	riboflavin synthase subunit alpha	0	NR-8043	E03
FTN_0109	-	-	hypothetical protein FTN_0109	0.2	NR-8048	G06
FTN_0546	-	COG1807M	dolichyl-phosphate-mannose-protein mannosyltransferase family protein	1.0	NR-8060	A06
FTN_1470	<i>ispA</i>	COG0142H	geranyl diphosphate synthase/farnesyl diphosphate synthase	2.0	NR-8058	F05
FTN_0113	<i>ribC</i>	COG0307H	riboflavin synthase subunit alph	4.0	NR-8060	C12
FTN_0545	-	COG0463M	glycosyl transferase	4.3	NR-8040	D09
FTN_1056	<i>clpX</i>	COG1219O	ATP-dependent protease ATP-binding subunit ClpX	5.1	NR-8061	H09
FTN_0545	-	COG0463M	glycosyl transferase	5.9	NR-8055	G11
FTN_0546	-	COG1807M	dolichyl-phosphate-mannose-protein mannosyltransferase family protein	11.9	NR-8050	D09
FTN_0296	<i>lysP</i>	COG0833E	lysine:H ⁺ symporter	28.5	NR-8058	A05
FTN_0417	<i>folD</i>	COG0190H	bifunctional 5,10-methylene-tetrahydrofolate dehydrogenase/ 5,10-methylene-tetrahydrofolate cyclohyd...	29.6	NR-8047	G04
FTN_0544	<i>naxD</i>	COG3394S	N-acetylhexosamine deacteylase	36.5	NR-8055	F02
FTN_0544	<i>naxD</i>	COG3394S	N-acetylhexosamine deacteylase	40.6	NR-8052	G01
FTN_0444	-	-	membrane protein	48.1	NR-8061	C10
FTN_0945	<i>rsuA</i>	COG1187J	16S rRNA pseudouridine synthase	50.1	NR-8064	E06
FTN_1240	-	COG0271T	hypothetical protein FTN_1240	50.7	NR-8058	C11
FTN_0444	-	-	membrane protein	51.4	NR-8047	C03
FTN_1313	-	-	hypothetical protein FTN_1313	52.5	NR-8046	F07
FTN_0416	<i>lpxE</i>	COG0671I	lipid A 1-phosphatase	52.6	NR-8043	E11
FTN_0561	<i>apaH</i>	COG0639T	diadenosine tetraphosphatase	53.7	NR-8056	H07
FTN_0599	-	-	hypothetical protein FTN_0599	55.6	NR-8052	G11
FTN_0515	<i>glgC</i>	COG0448G	glucose-1-phosphate adenylyltransferase	55.6	NR-8046	F05
FTN_1597	<i>prfC</i>	COG4108J	peptide chain release factor 3	57.0	NR-8063	F06
FTN_0178	<i>purA</i>	COG0104F	adenylosuccinate synthetase	57.0	NR-8037	A05

FTN_0554	-	COG0219J	RNA methyltransferase	57.3	NR-8049	F08
FTN_1551	<i>ampD</i>	COG3023V	N-acetyl-anhydromuranmyl-L-alanine amidase	57.8	NR-8048	E10
FTN_0178	<i>purA</i>	COG0104F	adenylosuccinate synthetase	59.2	NR-8065	G11
FTN_1091	<i>aroA</i>	COG0128E	3-phosphoshikimate 1-carboxyvinyltransferase	59.4	NR-8064	E08
FTN_1277	-	COG1538MU	outer membrane efflux protein	59.5	NR-8049	G08
FTN_1427	<i>wbtD</i>	COG0438M	group 1 glycosyl transferase	59.5	NR-8065	G01
FTN_0806	-	COG1472G	glycosyl hydrolase family protein	60.0	NR-8065	C03
FTN_1633	<i>apt</i>	COG0503F	adenine phosphoribosyltransferase	60.2	NR-8064	G01
FTN_0427	-	-	hypothetical protein FTN_0427	60.6	NR-8036	D12
FTN_0513	<i>glgB</i>	COG0296G	glycogen branching protein	60.9	NR-8066	D01
FTN_0719	-	-	hypothetical protein FTN_0719	60.9	NR-8047	A05
FTN_1715	<i>kdpD</i>	COG2205T	two component regulator, sensor histidine kinase kdpD	61.7	NR-8065	D11
FTN_0416	<i>lpxE</i>	COG0671I	lipid A 1-phosphatase	61.8	NR-8054	B11
FTN_0514	<i>pgm</i>	COG0033G	phosphoglucomutase	61.9	NR-8064	H04
FTN_0021	<i>carA</i>	COG0505EF	carbamoyl phosphate synthase small subunit	62.4	NR-8064	D08
FTN_0494	-	-	hypothetical protein FTN_0494	62.6	NR-8036	D02
FTN_0594	<i>sucC</i>	COG0045C	succinyl-CoA synthetase subunit beta	63.5	NR-8040	G06
FTN_0300	-	COG1215M	glycosyl transferase	63.5	NR-8060	F06
FTN_1219	<i>galE</i>	COG1087M	UDP-glucose 4-epimerase	63.7	NR-8064	C10
FTN_0132	-	-	hypothetical protein FTN_0132	63.9	NR-8036	A02
FTN_1057	<i>clpP</i>	COG07400U	ATP-dependent Clp protease proteolytic subunit	64.1	NR-8044	E02
FTN_1111	-	COG0769M	Mur ligase family protein	64.3	NR-8054	B01
FTN_1240	-	COG0271T	hypothetical protein FTN_1240	64.4	NR-8049	E10
FTN_1254	-	-	hypothetical protein FTN_1254	64.7	NR-8065	C05
FTN_0331	<i>minC</i>	COG0850D	septum site-determining protein MinC	64.9	NR-8060	F09
FTN_0945	<i>rsuA</i>	COG1187J	16S rRNA pseudouridine synthase	65.0	NR-8047	E08
FTN_0848	-	COG0531E	amino acid antiporter	65.0	NR-8054	C07
FTN_0669	<i>deoD</i>	COG0813F	purine nucleoside phosphorylase	65.0	NR-8065	E02
FTN_1213	-	COG1215M	glycosyl transferase family protein	65.5	NR-8066	D03
FTN_0296	<i>lysP</i>	COG0833E	lysine:H ⁺ symporter	65.7	NR-8058	B04
FTN_0506	<i>gcvH</i>	COG0509E	glycine cleavage system H protein	65.7	NR-8061	C05

FTN_0197	<i>cyoC</i>	COG1845C	cytochrome bo terminal oxidase subunit III	65.7	NR-8056	C11
FTN_1699	<i>purL</i>	COG0046F	phosphoribosylformylglycinamide synthase	66.0	NR-8065	E03
FTN_0494	-	-	hypothetical protein FTN_0494	66.5	NR-8057	B06
FTN_1500	-	-	hypothetical protein FTN_1500	66.5	NR-8064	C05
FTN_0672	<i>secA</i>	COG0653U	preprotein translocase subunit SecA	66.8	NR-8046	G03
FTN_0816	<i>bioA</i>	COG0161H	adenosylmethionine-8-amino-7-oxononanoate aminotransferase	66.8	NR-8047	H01
FTN_0495	-	COG4692G	BNR/Asp-box repeat-containing protein	67.0	NR-8048	H03
FTN_1311	-	-	hypothetical protein FTN_1311	67.0	NR-8051	G10
FTN_1357	<i>recB</i>	COG1074L	ATP-dependent exonuclease V subunit beta	67.2	NR-8053	B08
FTN_1056	<i>clpX</i>	COG1219O	ATP-dependent protease ATP-binding subunit ClpX	67.3	NR-8036	A06
FTN_0561	<i>apaH</i>	COG0639T	diadenosine tetraphosphatase	67.4	NR-8056	H07
FTN_1551	<i>ampD</i>	COG3023V	N-acetyl-anhydromuranmyl-L-alanine amidase	67.7	NR-8066	E04
FTN_0296	<i>lysP</i>	COG0833E	lysine:H ⁺ symporter	67.7	NR-8046	E12
FTN_1425	<i>wbtF</i>	COG0451MG	NAD dependent epimerase	67.8	NR-8066	E05
FTN_1272	-	COG3104E	proton-dependent oligopeptide transporter (POT) family protein, di- or tripeptide:H ⁺ symporter	68.0	NR-8050	B10
FTN_0202	<i>pdxY</i>	COG2240H	pyridoxal kinase	68.1	NR-8054	D06
FTN_1066	-	COG4535P	HlyC/CorC family transporter-associated protein	68.2	NR-8062	G03
FTN_1146	-	COG0436E	aspartate aminotransferase	68.2	NR-8036	B07
FTN_0842	<i>aroG</i>	COG0722E	phospho-2-dehydro-3-deoxyheptonate aldolase	68.3	NR-8066	G04
FTN_0436	-	COG3240IR	hypothetical protein FTN_0436	68.4	NR-8062	C03
FTN_0848	-	COG0531E	amino acid antiporter	68.4	NR-8036	D05
FTN_0298	<i>glpX</i>	COG1494G	fructose 1,6-bisphosphatase II	68.5	NR-8056	D09
FTN_1762	-	COG0488R	putative ABC transporter ATP-binding protein	68.5	NR-8058	F09
FTN_0036	<i>pyrD</i>	COG0167F	dihydroorotate oxidase	68.7	NR-8066	G12
FTN_1518	<i>relA</i>	COG0317TK	GDP pyrophosphokinase/GTP pyrophosphokinase	68.7	NR-8055	F10
FTN_1091	<i>aroA</i>	COG0128E	3-phosphoshikimate 1-carboxyvinyltransferase	68.7	NR-8058	D09
FTN_0434	<i>parB</i>	COG1475K	chromosome partition protein B	68.8	NR-8065	H12
FTN_0019	<i>pyrB</i>	COG0540F	aspartate carbamoyltransferase	68.9	NR-8037	C03
FTN_0098	<i>gidB</i>	COG0357M	16S rRNA methyltransferase GidB	69.0	NR-8055	D05
FTN_0651	<i>cdd</i>	COG0295F	cytidine deaminase	69.0	NR-8055	D09

FTN_0422	<i>purE</i>	COG0041F	N5-carboxyaminoimidazole ribonucleotide mutase	69.0	NR-8066	H09
FTN_0998	-	COG2898S	potassium channel protein	69.0	NR-8059	C12
FTN_1470	<i>ispA</i>	COG0142H	geranyl diphosphate synthase/farnesyl diphosphate synthase	69.2	NR-8046	B03
FTN_1107	<i>metI</i>	COG1464P	methionine uptake transporter (MUT) family protein, membrane and periplasmic protein	69.7	NR-8054	G08
FTN_0098	<i>gidB</i>	COG0357M	16S rRNA methyltransferase GidB	69.8	NR-8046	C06
FTN_0757	<i>cas9</i>	-	CRISPR/Cas associated protein	69.9	NR-8058	H09
FTN_1715	<i>kdpD</i>	COG2205T	two component regulator, sensor histidine kinase kdpD	69.9	NR-8043	H03
FTN_1038	-	COG0670R	hypothetical protein FTN_1038	70.0	NR-8056	H01
FTN_0177	<i>purH</i>	COG0138F	bifunctional phosphoribosylaminoimidazolecarboxamide formyltransferase/IMP cyclohydrolase	70.1	NR-8046	D12
FTN_0554	-	COG0219J	RNA methyltransferase	70.1	NR-8066	A05
FTN_1317	-	-	hypothetical protein FTN_1317	70.2	NR-8062	E10
FTN_0757	<i>cas9</i>	-	CRISPR/Cas associated protein	70.3	NR-8056	D11
FTN_1743	<i>clpB</i>	COG0542O	chaperone clpB	70.5	NR-8064	F04
FTN_1201	<i>capB</i>	COG0769M	capsule biosynthesis protein CapB	70.7	NR-8053	E03
FTN_0421	<i>purN</i>	COG0299F	phosphoribosylglycinamide formyltransferase	70.8	NR-8064	D04
FTN_1055	<i>lon</i>	COG0466O	DNA-binding, ATP-dependent protease La	70.8	NR-8045	E04
FTN_1199	-	-	hypothetical protein FTN_1199	70.9	NR-8054	G10
FTN_1314	-	-	hypothetical protein FTN_1314	70.9	NR-8054	A06
FTN_0330	<i>minD</i>	COG2894D	septum site-determining protein MinD	71.0	NR-8043	D01
FTN_0999	<i>udhA</i>	COG1249C	soluble pyridine nucleotide transhydrogenase	71.0	NR-8053	G08
FTN_1057	<i>clpP</i>	COG0740OU	ATP-dependent Clp protease proteolytic subunit	71.3	NR-8057	D05
FTN_1538	<i>groEL</i>	COG0459O	chaperonin GroEL	71.5	NR-8047	E04
FTN_0515	<i>glgC</i>	COG0448G	glucose-1-phosphate adenylyltransferase	71.6	NR-8065	C02
FTN_1315	-	-	hypothetical protein FTN_1315	71.8	NR-8062	A05
FTN_0325	-	COG2854Q	membrane protein	71.9	NR-8053	E09
FTN_0593	<i>sucD</i>	COG0074C	succinyl-CoA synthetase, alpha subunit	72.0	NR-8044	A06
FTN_0507	<i>gcvPI</i>	COG0403E	glycine dehydrogenase subunit 1	72.2	NR-8063	H03

FTN_1745	<i>purT</i>	COG0027F	phosphoribosylglycinamide formyltransferase 2	72.2	NR-8063	H08
FTN_1133	-	-	Ohr-like protein	72.3	NR-8046	E04
FTN_1357	<i>recB</i>	COG1074L	ATP-dependent exonuclease V subunit beta	72.3	NR-8042	E09
FTN_1064	-	COG1702T	PhoH family protein ATPase	72.5	NR-8035	A04
FTN_0772	-	COG0545O	hypothetical protein FTN_0772	72.5	NR-8056	C02
FTN_1421	<i>wbtH</i>	COG0367E	glutamine amidotransferase/asparagine synthase	72.5	NR-8062	H02
FTN_1016	-	COG1335Q	hypothetical protein FTN_1016	72.6	NR-8056	F09
FTN_0419	<i>purM</i>	COG0150F	phosphoribosylaminoimidazole synthetase	72.6	NR-8064	D05
FTN_0132	-	-	hypothetical protein FTN_0132	72.8	NR-8036	C02
FTN_0177	<i>purH</i>	COG0138F	bifunctional phosphoribosylaminoimidazolecarboxamide formyltransferase/IMP cyclohydrolase	72.8	NR-8065	F08
FTN_0097	-	COG0814E	hydroxy/aromatic amino acid permease (HAAAP) family protein	73.0	NR-8048	F08
FTN_1263	<i>comL</i>	COG4105R	competence lipoprotein ComL	73.0	NR-8048	G09
FTN_0331	<i>minC</i>	COG0850D	septum site-determining protein MinC	73.0	NR-8042	F06
FTN_0814	<i>bioF</i>	COG0156H	8-amino-7-oxononanoate synthase	73.1	NR-8056	F05
FTN_1317	-	-	hypothetical protein FTN_1317	73.1	NR-8036	B06
FTN_0690	<i>deaD</i>	COG0513LKJ	DEAD/DEAH box helicase	73.3	NR-8060	D08
FTN_1212	-	COG0438M	glycosyl transferases group 1 family protein	73.3	NR-8062	A01
FTN_0021	<i>carA</i>	COG0505EF	carbamoyl phosphate synthase small subunit	73.3	NR-8046	A09
FTN_0196	<i>cyoB</i>	COG0843C	cytochrome bo terminal oxidase subunit I	73.4	NR-8052	E03
FTN_0728	-	COG0053P	Co/Zn/Cd cation transporter	73.4	NR-8047	G03
FTN_0594	<i>sucC</i>	COG0045C	succinyl-CoA synthetase subunit beta	73.5	NR-8057	E02
FTN_1513	<i>xerC</i>	COG4973L	site-specific recombinase	73.6	NR-8048	E09
FTN_1254	-	-	hypothetical protein FTN_1254	73.6	NR-8066	C05
FTN_0358	<i>rimO</i>	COG0621J	ribosomal protein S12 methylthiotransferase	73.7	NR-8055	E09
FTN_1471	<i>pcs</i>	COG1183I	phosphatidylethanolamine synthase	73.8	NR-8040	D11
FTN_1700	<i>purF</i>	COG0034F	amidophosphoribosyltransferase	73.8	NR-8055	B12
FTN_1058	<i>tig</i>	COG0544O	trigger factor	74.0	NR-8053	B10
FTN_1217	-	COG1132V	ABC transporter ATP-binding protein	74.0	NR-8053	G01
FTN_0624	-	COG0814E	serine permease	74.0	NR-8064	H07

FTN_0855	-	-	hypothetical protein FTN_0855	74.0	NR-8062	D10
FTN_1211	-	COG1011R	haloacid dehalogenase-like hydrolase	74.2	NR-8053	G04
FTN_1316	-	COG3455S	hypothetical protein FTN_1316	74.2	NR-8055	A04
FTN_0534	-	COG1289S	hypothetical protein FTN_0534	74.4	NR-8054	H05
FTN_0815	<i>bioB</i>	COG0502H	biotin synthase	74.4	NR-8056	B10
FTN_1610	-	COG0841V	RND efflux transporter	74.4	NR-8054	B03
FTN_1602	<i>deoB</i>	COG1015G	phosphopentomutase	74.5	NR-8051	B10
FTN_0436	-	COG3240IR	hypothetical protein FTN_0436	74.6	NR-8040	H04
FTN_1055	<i>lon</i>	COG0466O	DNA-binding, ATP-dependent protease La	74.7	NR-8051	E07
FTN_1312	-	-	hypothetical protein FTN_1312	74.7	NR-8048	D06
FTN_1653	-	-	hypothetical protein FTN_1653	74.7	NR-8047	A11
FTN_1323	<i>iglB</i>	COG3517S	intracellular growth locus protein B	74.7	NR-8055	A06
FTN_1655	<i>rluC</i>	COG0564J	ribosomal large subunit pseudouridine synthase C	75.0	NR-8064	A09
FTN_1684	-	COG0019E	diaminopimelate decarboxylase	75.0	NR-8064	C12
FTN_0183	-	COG0803P	periplasmic solute binding family protein	75.0	NR-8055	A09
FTN_0822	-	COG0147EH	para-aminobenzoate synthase component I	75.1	NR-8040	C06
FTN_0298	<i>glpX</i>	COG1494G	fructose 1,6-bisphosphatase II	75.2	NR-8047	D09
FTN_0624	-	COG0814E	serine permease	75.3	NR-8054	A08
FTN_0666	<i>uvrA</i>	COG0178L	excinuclease ABC subunit A	75.5	NR-8066	D09
FTN_1558	<i>xerD</i>	COG4974L	site-specific recombinase	75.5	NR-8043	C10
FTN_0096	-	COG3619S	hypothetical protein FTN_0096	75.6	NR-8048	E08
FTN_0429	-	COG4372S	hypothetical protein FTN_0429	75.6	NR-8048	G12
FTN_0506	<i>gcvH</i>	COG0509E	glycine cleavage system H protein	75.6	NR-8049	G01
FTN_1066	-	COG4535P	HlyC/CorC family transporter-associated protein	75.7	NR-8045	B05
FTN_1091	<i>aroA</i>	COG0128E	3-phosphoshikimate 1-carboxyvinyltransferase	75.8	NR-8046	A01
FTN_0109	-	-	hypothetical protein FTN_0109	76.0	NR-8054	E12
FTN_0122	<i>recA</i>	COG0468L	recombinase A	76.0	NR-8035	D07
FTN_1500	-	-	hypothetical protein FTN_1500	76.3	NR-8048	C07
FTN_1313	-	-	hypothetical protein FTN_1313	76.4	NR-8057	F02
FTN_0122	<i>recA</i>	COG0468L	recombinase A	76.5	NR-8066	E09
FTN_1050	<i>hflX</i>	COG2262R	protease, GTP-binding subunit	76.6	NR-8058	A04
FTN_1097	-	COG1335Q	isochorismatase hydrolase family protein	76.6	NR-8054	F03

FTN_1200	<i>capC</i>	-	capsule biosynthesis protein CapC	76.6	NR-8052	G05
FTN_1318	-	-	hypothetical protein FTN_1318	76.6	NR-8054	F08
FTN_1558	<i>xerD</i>	COG4974L	site-specific recombinase	76.6	NR-8053	A03
FTN_0504	-	COG1982E	lysine decarboxylase	76.6	NR-8066	D07
FTN_0289	<i>proQ</i>	COG3109T	activator of osmoprotectant transporter ProP	76.7	NR-8036	D01
FTN_0821	-	COG0318IQ	AMP-binding protein	76.8	NR-8036	E05
FTN_0728	-	COG0053P	Co/Zn/Cd cation transporter	76.9	NR-8053	A07
FTN_1617	-	COG0642T	two-component regulator, sensor histidine kinase	76.9	NR-8054	A01
FTN_1133	-	-	Ohr-like protein	76.9	NR-8059	G08
FTN_1582	-	-	hypothetical protein FTN_1582	76.9	NR-8060	B01
FTN_0358	<i>rimO</i>	COG0621J	ribosomal protein S12 methylthiotransferase	77.0	NR-8048	E03
FTN_0330	<i>minD</i>	COG2894D	septum site-determining protein MinD	77.1	NR-8043	C09
FTN_1277	-	COG1538MU	outer membrane efflux protein	77.2	NR-8054	F05
FTN_1608	<i>dsbB</i>	COG1495O	disulfide bond formation protein	77.3	NR-8064	A08
FTN_0210	-	-	hypothetical protein FTN_0210	77.3	NR-8042	E07
FTN_0419	<i>purM</i>	COG0150F	phosphoribosylaminoimidazole synthetase	77.4	NR-8042	E12
FTN_0495	-	COG4692G	BNR/Asp-box repeat-containing protein	77.4	NR-8061	D05
FTN_1107	<i>metIQ</i>	COG1464P	methionine uptake transporter (MUT) family protein, membrane and periplasmic protein	77.4	NR-8065	F04
FTN_0119	-	COG2825M	hypothetical protein FTN_0119	77.5	NR-8057	D03
FTN_1146	-	COG0436E	aspartate aminotransferase	77.5	NR-8057	B10
FTN_0337	<i>fumA</i>	COG1951C	fumerate hydratase	77.6	NR-8045	D06
FTN_1699	<i>purL</i>	COG0046F	phosphoribosylformylglycinamide synthase	77.6	NR-8040	D02
FTN_1242	-	COG0586S	DedA family protein	77.6	NR-8052	B12
FTN_0234	<i>pgsA</i>	COG0558I	phosphatidylglycerophosphate synthetase	77.6	NR-8040	B01
FTN_0720	-	COG1414K	IclR family transcriptional regulator	77.6	NR-8054	G01
FTN_1750	-	COG0204I	acyltransferase	77.7	NR-8044	B05
FTN_0297	-	COG2945R	hypothetical protein FTN_0297	77.8	NR-8062	B05
FTN_1318	-	-	hypothetical protein FTN_1318	77.8	NR-8048	H06
FTN_1209	<i>cphB</i>	COG4242QP	cyanophycinase	77.8	NR-8055	F05
FTN_1362	-	-	hypothetical protein FTN_1362	77.9	NR-8055	E08
FTN_1362	-	-	hypothetical protein FTN_1362	78.0	NR-8038	G09

FTN_1322	<i>iglC</i>	-	intracellular growth locus protein C	78.1	NR-8052	H02
FTN_1426	<i>wbtE</i>	COG0677M	UDP-glucose/GDP-mannose dehydrogenase	78.1	NR-8054	H10
FTN_0728	-	COG0053P	Co/Zn/Cd cation transporter	78.1	NR-8048	H04
FTN_1326	<i>anmK</i>	COG2377O	anhydro-N-acetylmuramic acid kinase	78.1	NR-8048	C11
FTN_0020	<i>carB</i>	COG0458EF	carbamoyl phosphate synthase large subunit	78.2	NR-8042	D03
FTN_0756	<i>fopA</i>	COG2885M	OmpA family protein	78.3	NR-8063	G12
FTN_1219	<i>galE</i>	COG1087M	UDP-glucose 4-epimerase	78.3	NR-8064	E10
FTN_1425	<i>wbtF</i>	COG0451MG	NAD dependent epimerase	78.3	NR-8040	E08
FTN_1219	<i>galE</i>	COG1087M	UDP-glucose 4-epimerase	78.3	NR-8050	C05
FTN_0210	-	-	hypothetical protein FTN_0210	78.4	NR-8042	D07
FTN_1613	-	COG1619V	U61 family peptidase	78.4	NR-8046	D11
FTN_1656	-	COG1485R	ATPase	78.5	NR-8050	B11
FTN_0664	<i>fimT</i>	COG4970NU	Type IV pili, pilus assembly protein	78.5	NR-8057	A06
FTN_1058	<i>tig</i>	COG0544O	trigger factor	78.6	NR-8040	A06
FTN_0560	<i>ksgA</i>	COG0030J	dimethyladenosine transferase	78.7	NR-8053	D06
FTN_0210	-	-	hypothetical protein FTN_0210	78.7	NR-8063	G07
FTN_1273	-	COG0318IQ	long chain fatty acid CoA ligase	78.8	NR-8066	A07
FTN_0427	-	-	hypothetical protein FTN_0427	78.9	NR-8054	A05
FTN_0429	-	COG4372S	hypothetical protein FTN_0429	78.9	NR-8053	F10
FTN_1090	-	-	hypothetical protein FTN_1090	79.0	NR-8036	C05
FTN_1264	<i>rluD</i>	COG0564J	ribosomal large subunit pseudouridine synthase D	79.0	NR-8065	C11
FTN_1201	<i>capB</i>	COG0769M	capsule biosynthesis protein CapB	79.0	NR-8044	C01
FTN_1617	-	COG0642T	two-component regulator, sensor histidine kinase	79.0	NR-8042	E05
FTN_0096	-	COG3619S	hypothetical protein FTN_0096	79.1	NR-8057	C09
FTN_1309	<i>pdpA</i>	-	hypothetical protein FTN_1309	79.1	NR-8065	E06
FTN_1029	-	COG3155Q	isoprenoid biosynthesis protein with amidotransferase-like domain	79.2	NR-8057	F06
FTN_0505	<i>gcvT</i>	COG0404E	glycine cleavage system aminomethyltransferase T	79.3	NR-8041	C06
FTN_1209	<i>cphB</i>	COG4242QP	cyanophycinase	79.4	NR-8038	E10
FTN_1048	<i>hflK</i>	COG0330O	HflK-HflC membrane protein complex, HflK	79.5	NR-8041	E03
FTN_0560	<i>ksgA</i>	COG0030J	dimethyladenosine transferase	79.5	NR-8056	C05

FTN_0689	<i>ppiC</i>	COG07600	parvulin-like peptidyl-prolyl isomerase domain-containing protein	79.6	NR-8059	D08
FTN_0534	-	COG1289S	hypothetical protein FTN_0534	79.6	NR-8047	F04
FTN_1513	<i>xerC</i>	COG4973L	site-specific recombinase	79.6	NR-8065	E12
FTN_1684	-	COG0019E	diaminopimelate decarboxylase	79.6	NR-8064	E12
FTN_1111	-	COG0769M	Mur ligase family protein	79.6	NR-8040	F04
FTN_0593	<i>sucD</i>	COG0074C	succinyl-CoA synthetase, alpha subunit	79.7	NR-8057	H02
FTN_0893	-	-	hypothetical protein FTN_0893	79.7	NR-8061	D08
FTN_1324	<i>igla</i>	COG3516S	intracellular growth locus protein A	79.7	NR-8061	A04
FTN_0690	<i>deaD</i>	COG0513LKJ	DEAD/DEAH box helicase	79.8	NR-8041	G12
FTN_1586	-	COG2814G	major facilitator superfamily sugar transporter	79.8	NR-8051	B07
FTN_1705	-	COG0826O	U32 family peptidase	79.8	NR-8047	E01
FTN_0672	<i>secA</i>	COG0653U	preprotein translocase subunit SecA	79.8	NR-8052	F04
FTN_1715	<i>kdpD</i>	COG2205T	two component regulator, sensor histidine kinase kdpD	79.8	NR-8055	B07
FTN_1064	-	COG1702T	PhoH family protein ATPase	79.9	NR-8061	E03
FTN_0514	<i>pgm</i>	COG0033G	phosphoglucomutase	80.1	NR-8045	C12
FTN_1218	-	COG0438M	group 1 glycosyl transferase	80.1	NR-8062	E08
FTN_1433	-	-	hypothetical protein FTN_1433	80.1	NR-8060	B06
FTN_0599	-	-	hypothetical protein FTN_0599	80.1	NR-8066	G06
FTN_1613	-	COG1619V	U61 family peptidase	80.1	NR-8057	H10
FTN_1313	-	-	hypothetical protein FTN_1313	80.4	NR-8043	D06
FTN_0494	-	-	hypothetical protein FTN_0494	80.4	NR-8063	C09
FTN_1038	-	COG0670R	hypothetical protein FTN_1038	80.4	NR-8036	D07
FTN_1382	-	-	hypothetical protein FTN_1382	80.6	NR-8055	C03
FTN_1548	<i>groEL</i>	COG0459O	chaperonin GroEL	80.6	NR-8040	B07
FTN_0818	-	COG0657I	lipase/esterase	80.6	NR-8036	D08
FTN_1316	-	COG3455S	hypothetical protein FTN_1316	80.6	NR-8040	F08
FTN_1097	-	COG1335Q	isochorismatase hydrolase family protein	80.7	NR-8052	A01
FTN_0756	<i>fopA</i>	COG2885M	OmpA family protein	80.7	NR-8061	H10
FTN_1048	<i>hflK</i>	COG0330O	HflK-HflC membrane protein complex, HflK	80.7	NR-8059	D12
FTN_1218	-	COG0438M	group 1 glycosyl transferase	80.8	NR-8041	C04

FTN_1319	<i>pdpC</i>	-	hypothetical protein FTN_1319	80.9	NR-8054	F01
FTN_0177	<i>purH</i>	COG0138F	bifunctional phosphoribosylaminoimidazolecarboxamide formyltransferase/IMP cyclohydrolase	80.9	NR-8040	H02
FTN_1242	-	COG0586S	DedA family protein	80.9	NR-8043	G08
FTN_1252	-	COG3049M	choloylglycine hydrolase family protein	81.1	NR-8058	G09
FTN_1257	-	-	hypothetical protein FTN_1257	81.1	NR-8057	B07
FTN_0855	-	-	hypothetical protein FTN_0855	81.2	NR-8047	A04
FTN_0407	-	COG0833E	amino acid ABC transporter permease	81.3	NR-8053	G07
FTN_0925	-	-	hypothetical protein FTN_0925	81.4	NR-8058	H11
FTN_1321	<i>iglD</i>	-	intracellular growth locus protein D	81.5	NR-8063	B02
FTN_1410	<i>bfr</i>	COG2193P	bacterioferritin	81.5	NR-8061	C12
FTN_0818	-	COG0657I	lipase/esterase	81.6	NR-8036	C08
FTN_0266	<i>htpG</i>	COG0326O	heat shock protein 90	81.6	NR-8050	F02
FTN_0325	-	COG2854Q	membrane protein	81.7	NR-8046	C03
FTN_1750	-	COG0204I	acyltransferase	81.8	NR-8064	A10
FTN_0297	-	COG2945R	hypothetical protein FTN_0297	81.8	NR-8042	C01
FTN_0643	-	-	hypothetical protein FTN_0643	81.9	NR-8055	A08
FTN_0842	<i>aroG</i>	COG0722E	phospho-2-dehydro-3-deoxyheptonate aldolase	82.0	NR-8041	G10
FTN_1501	-	COG0025P	monovalent cation:proton antiporter-1	82.0	NR-8045	E10
FTN_1157	-	COG1217T	GTP binding translational elongation factor Tu and G family protein	82.0	NR-8061	D10
FTN_0817	-	COG2050Q	hypothetical protein FTN_0817	82.1	NR-8040	F09
FTN_1597	<i>prfC</i>	COG4108J	peptide chain release factor 3	82.1	NR-8043	F01
FTN_0544	<i>naxD</i>	COG3394S	galactosamine deacetylase	82.2	NR-8062	D08
FTN_0756	<i>fopA</i>	COG2885M	OmpA family protein	82.2	NR-8038	G11
FTN_1633	<i>apt</i>	COG0503F	adenine phosphoribosyltransferase	82.2	NR-8035	B09
FTN_0020	<i>carB</i>	COG0458EF	carbamoyl phosphate synthase large subunit	82.3	NR-8043	B03
FTN_0505	<i>gcvT</i>	COG0404E	glycine cleavage system aminomethyltransferase T	82.3	NR-8045	E03
FTN_1745	<i>purT</i>	COG0027F	phosphoribosylglycinamide formyltransferase 2	82.3	NR-8050	E09
FTN_1548	-	COG1520S	hypothetical protein FTN_1548	82.4	NR-8043	A01
FTN_1657	-	COG2271G	major facilitator transporter	82.5	NR-8052	G02

FTN_1319	<i>pdpC</i>	-	hypothetical protein FTN_1319	82.5	NR-8035	G09
FTN_0507	<i>gcvPI</i>	COG0403E	glycine dehydrogenase subunit 1	82.6	NR-8040	E04
FTN_0822	-	COG0147EH	para-aminobenzoate synthase component I	82.7	NR-8062	H01
FTN_1320	-	-	hypothetical protein FTN_1320	82.7	NR-8059	E10
FTN_1744	<i>chiB</i>	COG3469G	chitinase	82.7	NR-8058	G04
FTN_0817	-	COG2050Q	hypothetical protein FTN_0817	82.7	NR-8051	A06
FTN_1656	-	COG1485R	ATPase	82.9	NR-8060	C04
FTN_0643	-	-	hypothetical protein FTN_0643	83.0	NR-8042	A02
FTN_0818	-	COG0657I	lipase/esterase	83.0	NR-8046	C10
FTN_1312	-	-	hypothetical protein FTN_1312	83.1	NR-8057	H04
FTN_0664	<i>fimT</i>	COG4970NU	Type IV pili, pilus assembly protein	83.1	NR-8045	C11
FTN_1586	-	COG2814G	major facilitator superfamily sugar transporter	83.1	NR-8043	B02
FTN_0633	<i>katG</i>	COG0376P	peroxidase/catalase	83.2	NR-8040	A05
FTN_1743	<i>clpB</i>	COG0542O	chaperone clpB	83.2	NR-8059	H05
FTN_1607	<i>cca</i>	COG0617J	tRNA CCA-pyrophosphorylase	83.3	NR-8046	G12
FTN_0624	-	COG0814E	serine permease	83.3	NR-8040	H08
FTN_0535	-	COG2814G	drug:H ⁺ antiporter-1 (DHA1) family protein	83.3	NR-8053	A09
FTN_0198	<i>cyoD</i>	COG3125C	cytochrome bo terminal oxidase subunit IV	83.4	NR-8061	F07
FTN_0593	<i>sucD</i>	COG0074C	succinyl-CoA synthetase, alpha subunit	83.4	NR-8061	B09
FTN_0422	<i>purE</i>	COG0041F	N5-carboxyaminoimidazole ribonucleotide mutase	83.4	NR-8042	F12
FTN_1438	-	COG1250I	fusion product of 3-hydroxacyl-CoA dehydrogenase and acyl-CoA-binding protein	83.4	NR-8041	E09
FTN_1050	<i>hflX</i>	COG2262R	protease, GTP-binding subunit	83.6	NR-8042	E08
FTN_1256	-	-	hypothetical protein FTN_1256	83.7	NR-8062	H12
FTN_1325	<i>pdpD</i>	-	hypothetical protein FTN_1325	83.7	NR-8058	H01
FTN_1654	-	COG2271G	major facilitator transporter	83.7	NR-8058	G07
FTN_1311	-	-	hypothetical protein FTN_1311	83.7	NR-8043	F12
FTN_0132	-	-	hypothetical protein FTN_0132	83.9	NR-8063	G03
FTN_1112	<i>cphA</i>	COG0769M	cyanophycin synthetase	83.9	NR-8061	B03
FTN_1263	<i>comL</i>	COG4105R	competence lipoprotein ComL	83.9	NR-8060	G10
FTN_1276	-	COG1566V	membrane fusion protein	83.9	NR-8061	A02
FTN_1682	<i>frgA</i>	COG4264Q	siderophore biosynthesis protein	83.9	NR-8058	H10

FTN_0812	<i>bioD</i>	COG0132H	dethiobiotin synthetase	84.0	NR-8051	C10
FTN_0719	-	-	hypothetical protein FTN_0719	84.0	NR-8039	G09
FTN_0925	-	-	hypothetical protein FTN_0925	84.0	NR-8045	G06
FTN_0097	-	COG0814E	hydroxy/aromatic amino acid permease (HAAAP) family protein	84.0	NR-8059	H10
FTN_0771	-	COG1651O	protein-disulfide isomerase	84.2	NR-8058	F12
FTN_1326	<i>anmK</i>	COG2377O	anhydro-N-acetylmuramic acid kinase	84.2	NR-8061	F03
FTN_1744	<i>chiB</i>	COG3469G	chitinase	84.3	NR-8045	D11
FTN_1058	<i>tig</i>	COG0544O	trigger factor	84.3	NR-8038	G01
FTN_1427	<i>wbtD</i>	COG0438M	group 1 glycosyl transferase	84.3	NR-8035	B05
FTN_0035	<i>pyrF</i>	COG0284F	orotidine-5'-phosphate decarboxylase	84.3	NR-8063	E04
FTN_1321	<i>iglD</i>	-	intracellular growth locus protein D	84.3	NR-8061	E05
FTN_0430	-	-	hypothetical protein FTN_0430	84.5	NR-8040	E09
FTN_1016	-	COG1335Q	hypothetical protein FTN_1016	84.6	NR-8043	A09
FTN_0211	<i>pcp</i>	COG2039O	pyrrolidone carboxylate peptidase	84.7	NR-8053	E10
FTN_0407	-	COG0833E	amino acid ABC transporter permease	84.8	NR-8041	F04
FTN_1657	-	COG2271G	major facilitator transporter	84.8	NR-8044	G09
FTN_0197	<i>cyoC</i>	COG1845C	cytochrome bo terminal oxidase subunit III	84.9	NR-8050	D07
FTN_0816	<i>bioA</i>	COG0161H	adenosylmethionine-8-amino-7-oxononanoate aminotransferase	85.0	NR-8060	E06
FTN_0666	<i>uvrA</i>	COG0178L	excinuclease ABC subunit A	85.0	NR-8045	E09
FTN_1211	-	COG1011R	haloacid dehalogenase-like hydrolase	85.1	NR-8035	E11
FTN_1427	<i>wbtD</i>	COG0438M	group 1 glycosyl transferase	85.2	NR-8058	D12
FTN_1310	<i>pdpB</i>	COG3523S	hypothetical protein FTN_1310	85.3	NR-8039	G10
FTN_1220	-	COG2148M	lipopolysaccharide synthesis sugar transferase	85.3	NR-8040	C12
FTN_1683	-	COG2814G	drug:H ⁺ antiporter-1 (DHA1) family protein	85.3	NR-8044	D12
FTN_0812	<i>bioD</i>	COG0132H	dethiobiotin synthetase	85.5	NR-8035	A12
FTN_1421	<i>wbtH</i>	COG0367E	glutamine amidotransferase/asparagine synthase	85.5	NR-8040	C03
FTN_1705	-	COG0826O	U32 family peptidase	85.5	NR-8062	G04
FTN_1007	<i>rplY</i>	COG1825J	50S ribosomal protein L25	85.6	NR-8036	H08
FTN_0019	<i>pyrB</i>	COG0540F	aspartate carbamoyltransferase	85.7	NR-8063	A02
FTN_0431	-	COG3307M	hypothetical protein FTN_0431	85.8	NR-8060	H05

FTN_1107	<i>metIQ</i>	COG1464P	methionine uptake transporter (MUT) family protein, membrane and periplasmic protein	86.1	NR-8044	A02
FTN_0266	<i>htpG</i>	COG0326O	heat shock protein 90	86.2	NR-8044	A08
FTN_1518	<i>relA</i>	COG0317TK	GDP pyrophosphokinase/GTP pyrophosphokinase	86.2	NR-8041	C09
FTN_0620	-	COG2271G	major facilitator transporter	86.3	NR-8058	C09
FTN_1277	-	COG1538MU	outer membrane efflux protein	86.3	NR-8063	D05
FTN_1548	-	COG1520S	hypothetical protein FTN_1548	86.5	NR-8061	F12
FTN_1426	<i>wbtE</i>	COG0677M	UDP-glucose/GDP-mannose dehydrogenase	86.5	NR-8045	H08
FTN_1750	-	COG0204I	acyltransferase	86.6	NR-8057	D04
FTN_1214	-	COG1215M	glycosyl transferase family protein	86.7	NR-8053	B07
FTN_1254	-	-	hypothetical protein FTN_1254	86.8	NR-8036	G07
FTN_0812	<i>bioD</i>	COG0132H	dethiobiotin synthetase	86.9	NR-8050	H08
FTN_0620	-	COG2271G	major facilitator transporter	86.9	NR-8035	E06
FTN_1157	-	COG1217T	GTP binding translational elongation factor Tu and G family protein	87.0	NR-8041	F11
FTN_0358	<i>rimO</i>	COG0621J	ribosomal protein S12 methylthiotransferase	87.1	NR-8045	G10
FTN_0731	-	COG5006R	hypothetical protein FTN_0731	87.1	NR-8044	D01
FTN_0410	-	COG0436E	aspartate aminotransferase	87.2	NR-8035	B06
FTN_0689	<i>ppiC</i>	COG0760O	parvulin-like peptidyl-prolyl isomerase domain-containing protein	87.2	NR-8035	B03
FTN_1090	-	-	hypothetical protein FTN_1090	87.3	NR-8052	C12
FTN_0823	<i>pabA</i>	COG0512EH	anthranilate synthase component II	87.4	NR-8035	H06
FTN_0120	-	COG0607P	rhodanese-related sulfurtransferase	87.5	NR-8053	A11
FTN_1431	<i>wbtA</i>	COG1086MG	dTDP-glucose 4,6-dehydratase	87.5	NR-8057	B09
FTN_1501	-	COG0025P	monovalent cation:proton antiporter-1	87.5	NR-8057	H12
FTN_1683	-	COG2814G	drug:H ⁺ antiporter-1 (DHA1) family protein	87.5	NR-8058	E01
FTN_1256	-	-	hypothetical protein FTN_1256	87.5	NR-8041	B06
FTN_0806	-	COG1472G	glycosyl hydrolase family protein	87.6	NR-8036	H01
FTN_1745	<i>purT</i>	COG0027F	phosphoribosylglycinamide formyltransferase 2	87.6	NR-8063	A05
FTN_0431	-	COG3307M	hypothetical protein FTN_0431	87.7	NR-8044	A10
FTN_0651	<i>cdd</i>	COG0295F	cytidine deaminase	87.8	NR-8051	D03
FTN_1315	-	-	hypothetical protein FTN_1315	87.8	NR-8048	G08

FTN_0410	-	COG0436E	aspartate aminotransferase	88.0	NR-8059	B07
FTN_1214	-	COG1215M	glycosyl transferase family protein	88.0	NR-8063	B10
FTN_1131	<i>putA</i>	COG4230C	bifunctional proline dehydrogenase/pyrroline-5-carboxylate dehydrogenase	88.1	NR-8044	C10
FTN_0289	<i>proQ</i>	COG3109T	activator of osmoprotectant transporter ProP	88.1	NR-8058	E05
FTN_1750	-	COG0204I	acyltransferase	88.3	NR-8053	H02
FTN_1682	<i>frgA</i>	COG4264Q	siderophore biosynthesis protein	88.4	NR-8047	B07
FTN_0183	-	COG0803P	periplasmic solute binding family protein	88.5	NR-8058	C01
FTN_0669	<i>deoD</i>	COG0813F	purine nucleoside phosphorylase	88.5	NR-8038	H09
FTN_0599	-	-	hypothetical protein FTN_0599	88.6	NR-8048	A10
FTN_1654	-	COG2271G	major facilitator transporter	88.6	NR-8050	A12
FTN_1438	-	COG1250I	fusion product of 3-hydroxacyl-CoA dehydrogenase and acyl-CoA-binding protein	88.6	NR-8052	F03
FTN_0999	<i>udhA</i>	COG1249C	soluble pyridine nucleotide transhydrogenase	88.7	NR-8035	G04
FTN_1214	-	COG1215M	glycosyl transferase family protein	88.7	NR-8048	A07
FTN_1159	<i>ggt</i>	COG0405E	gamma-glutamyltranspeptidase	88.9	NR-8050	H10
FTN_0202	<i>pdxY</i>	COG2240H	pyridoxal kinase	89.0	NR-8039	D03
FTN_0430	-	-	hypothetical protein FTN_0430	89.1	NR-8057	F04
FTN_0643	-	-	hypothetical protein FTN_0643	89.1	NR-8051	F07
FTN_1323	<i>iglB</i>	COG3517S	intracellular growth locus protein B	89.3	NR-8044	G02
FTN_1582	-	-	hypothetical protein FTN_1582	89.3	NR-8042	E11
FTN_1610	-	COG0841V	RND efflux transporter	89.5	NR-8036	G04
FTN_0814	<i>bioF</i>	COG0156H	8-amino-7-oxononanoate synthase	89.9	NR-8041	E11
FTN_0513	<i>glgB</i>	COG0296G	glycogen branching protein	90.0	NR-8039	F12
FTN_0633	<i>katG</i>	COG0376P	peroxidase/catalase	90.0	NR-8052	D04
FTN_1273	-	COG0318IQ	long chain fatty acid CoA ligase	90.0	NR-8048	B09
FTN_1252	-	COG3049M	choloylglycine hydrolase family protein	90.3	NR-8038	E09
FTN_1423	<i>wbtG</i>	COG0438M	group 1 glycosyl transferase	90.4	NR-8051	F12
FTN_0036	<i>pyrD</i>	COG0167F	dihydroorotate oxidase	90.5	NR-8037	D06
FTN_0561	<i>apaH</i>	COG0639T	diadenosine tetraphosphatase	90.7	NR-8039	C12
FTN_0120	-	COG0607P	rhodanese-related sulfurtransferase	90.9	NR-8050	A04
FTN_1310	<i>pdpB</i>	COG3523S	hypothetical protein FTN_1310	90.9	NR-8052	A09

FTN_1325	<i>pdpD</i>	-	hypothetical protein FTN_1325	91.1	NR-8036	F02
FTN_1276	-	COG1566V	membrane fusion protein	91.5	NR-8064	C03
FTN_1213	-	COG1215M	glycosyl transferase family protein	92.0	NR-8037	D07
FTN_1518	<i>relA</i>	COG0317TK	GDP pyrophosphokinase/GTP pyrophosphokinase	92.1	NR-8040	B02
FTN_1322	<i>iglC</i>	-	intracellular growth locus protein C	92.4	NR-8048	G02
FTN_1357	<i>recB</i>	COG1074L	ATP-dependent exonuclease V subunit beta	92.4	NR-8038	H07
FTN_1324	<i>iglA</i>	COG3516S	intracellular growth locus protein A	92.8	NR-8039	C08
FTN_1431	<i>wbtA</i>	COG1086MG	dTDP-glucose 4,6-dehydratase	92.8	NR-8040	G03
FTN_0731	-	COG5006R	hypothetical protein FTN_0731	93.1	NR-8037	F11
FTN_1257	-	-	hypothetical protein FTN_1257	93.3	NR-8037	B01
FTN_1220	-	COG2148M	lipopolysaccharide synthesis sugar transferase	93.6	NR-8061	G05
FTN_0505	<i>gcvT</i>	COG0404E	glycine cleavage system aminomethyltransferase T	93.6	NR-8037	D04
FTN_1743	<i>clpB</i>	COG0542O	chaperone clpB	93.7	NR-8045	F03
FTN_0211	<i>pcp</i>	COG2039O	pyrrolidone carboxylate peptidase	93.9	NR-8038	B01
FTN_0561	<i>apaH</i>	COG0639T	diadenosine tetraphosphatase	93.9	NR-8039	C12
FTN_1159	<i>ggt</i>	COG0405E	gamma-glutamyltranspeptidase	94.1	NR-8051	F06
FTN_1762	-	COG0488R	putative ABC transporter ATP-binding protein	94.1	NR-8046	E09
FTN_1112	<i>cphA</i>	COG0769M	cyanophycin synthetase	94.1	NR-8045	H04
FTN_1199	-	-	hypothetical protein FTN_1199	94.2	NR-8038	C05
FTN_0823	<i>pabA</i>	COG0512EH	anthranilate synthase component II	94.2	NR-8052	B05
FTN_1655	<i>rluC</i>	COG0564J	ribosomal large subunit pseudouridine synthase C	94.4	NR-8038	D08
FTN_1682	<i>frgA</i>	COG4264Q	siderophore biosynthesis protein	94.4	NR-8038	G04
FTN_1410	<i>bfr</i>	COG2193P	bacterioferritin	94.6	NR-8047	B12
FTN_1417	<i>manB</i>	COG1109G	phosphomannomutase	94.7	NR-8065	F11
FTN_1684	-	COG0019E	diaminopimelate decarboxylase	94.9	NR-8045	B09
FTN_0720	-	COG1414K	IclR family transcriptional regulator	94.9	NR-8038	A11
FTN_0265	<i>rplQ</i>	COG0203J	50S ribosomal protein L17	95.2	NR-8037	E11
FTN_1602	<i>deoB</i>	COG1015G	phosphopentomutase	95.5	NR-8038	E05
FTN_1255	-	COG1442M	glycosyl transferase family protein	95.7	NR-8039	C11
FTN_0535	-	COG2814G	drug:H ⁺ antiporter-1 (DHA1) family protein	96.2	NR-8038	B04
FTN_0815	<i>bioB</i>	COG0502H	biotin synthase	96.3	NR-8037	G05

FTN_1029	-	COG3155Q	isoprenoid biosynthesis protein with amidotransferase-like domain	96.3	NR-8038	F11
FTN_1264	<i>rluD</i>	COG0564J	ribosomal large subunit pseudouridine synthase D	96.6	NR-8038	G05
FTN_1683	-	COG2814G	drug:H ⁺ antiporter-1 (DHA1) family protein	96.7	NR-8037	G08
FTN_1254	-	-	hypothetical protein FTN_1254	97.2	NR-8036	H07
FTN_1608	<i>dsbB</i>	COG1495O	disulfide bond formation protein	97.2	NR-8039	A10
FTN_0035	<i>pyrF</i>	COG0284F	orotidine-5'-phosphate decarboxylase	97.3	NR-8038	D10
FTN_0196	<i>cyoB</i>	COG0843C	cytochrome bo terminal oxidase subunit I	98.0	NR-8039	B03
FTN_0504	-	COG1982E	lysine decarboxylase	98.8	NR-8039	B11
FTN_1683	-	COG2814G	drug:H ⁺ antiporter-1 (DHA1) family protein	98.9	NR-8052	E12
FTN_1212	-	COG0438M	glycosyl transferases group 1 family protein	99.1	NR-8039	F08
FTN_0893	-	-	hypothetical protein FTN_0893	99.4	NR-8037	E12
FTN_1423	<i>wbtG</i>	COG0438M	group 1 glycosyl transferase	99.4	NR-8037	A12
FTN_0198	<i>cyoD</i>	COG3125C	cytochrome bo terminal oxidase subunit IV	99.9	NR-8046	F12
FTN_0421	<i>purN</i>	COG0299F	phosphoribosylglycinamide formyltransferase	100.6	NR-8038	C03
FTN_0813	<i>bioC</i>	-	biotin synthesis protein BioC	101.2	NR-8038	H12
FTN_0998	-	COG2898S	potassium channel protein	101.2	NR-8039	D11
FTN_1320	-	-	hypothetical protein FTN_1320	101.2	NR-8037	H05
FTN_0487	<i>rpsU</i>	COG0828J	30S ribosomal protein S21	101.4	NR-8038	A01
FTN_1217	-	COG1132V	ABC transporter ATP-binding protein	101.4	NR-8038	G03
FTN_1309	<i>pdpA</i>	-	hypothetical protein FTN_1309	101.4	NR-8039	D04
FTN_1433	-	-	hypothetical protein FTN_1433	104.8	NR-8039	F07
FTN_1131	<i>putA</i>	COG4230C	bifunctional proline dehydrogenase/pyrroline-5-carboxylate dehydrogenase	105.4	NR-8038	G10
FTN_1412	-	COG0202K	DNA-directed RNA polymerase subunit alpha	105.4	NR-8038	D11
FTN_1417	<i>manB</i>	COG1109G	phosphomannomutase	105.9	NR-8050	G02
FTN_1314	-	-	hypothetical protein FTN_1314	111.5	NR-8037	G10
FTN_1309	<i>pdpA</i>	-	hypothetical protein FTN_1309	123.5	NR-8039	F04

Supplemental Table 3. Primers used in this study

<i>Primer name</i>	<i>Sequence</i>
0109 Arm1 FWD	caccagttttaaagaggt
0109 Arm 1 REV	ttatcgataccgtcgacctcactaaatttccatgatttaataac
0109 frt_sKAN_frt FWD	gttattaaatcatggaaatttagtgaggctgacggatcgataa
0109 frt_sKAN_frt REV	ttatttaggattacttatttaatttgcatagctgcaggatcgata
0109 Arm 2 FWD	tatcgatcctgcagctatgcaaattaaataagtaatcctaataa
0109 Arm 2 REV	ttcctataggcaacattga
0430 Arm1 FWD	ttacttagatactctagctg
0430 Arm 1 REV	ttatcgataccgtcgacctctagtattacctgttatttcatta
0430 frt_sKAN_frt FWD	taatgaataaacaggttaatactagaggtcgacggatcgataa
0430 frt_sKAN_frt REV	tcttataaaaagacggcaaaaagcatagctgcaggatcgata
0430 Arm 2 FWD	tatcgatcctgcagctatgctttttgccgtctttataaga
0430 Arm 2 REV	aaaatcgtactgctttagaat